Sains Malaysiana 52(3)(2023): 899-939
*http://doi.org/10.17576/jsm-2023-5203-17*

# Exploration of *Annona muricata* (Annonaceae) in the Treatment of Hyperlipidemia Through Network Pharmacology and Molecular Docking

(Penerokaan *Annona muricata* (Annonaceae) dalam Rawatan Hiperlipidemia Melalui Rangkaian Farmakologi dan Dok Molekul)

Reny Syahruni[1], Abdul Halim Umar[1,*], Hindriyani Nurul Rahman[1] & Wisnu Ananta Kusuma[2]

[1]*Division of Pharmaceutical Biology, College of Pharmaceutical Sciences Makassar (Sekolah Tinggi Ilmu Farmasi Makassar), Jalan Perintis Kemerdekaan Km. 13.7 Daya, Makassar 90242, Indonesia*
[2]*Department of Computer Science, Faculty of Mathematics and Natural Sciences, Jalan Meranti-Dramaga Campus, IPB University, Bogor 16680, Indonesia*

*Received: 11 August 2022/Accepted: 5 January 2023*

ABSTRACT

Soursop (*Annona muricata* L.) is one of the plants that have antihyperlipidemic effects, but its underlying mechanism of action remains unknown. Previous investigations used TCMSP, KNApSAcK, ETCM, SwissTargetPrediction, SuperPred, CTD, and TTD to identify potential targets of soursop as antihyperlipidemic. Therefore, this study aims to explore soursop active compounds and demonstrate their mechanisms against hyperlipidemia through network pharmacology and molecular docking. OB and drug-likeness properties of the compounds from *A. muricata* were screened based on Lipinski's Ro5 (Lipinski's Rule of Five) parameters. Subsequently, the network of the compound–target–disease–pathways was constructed using Cytoscape. The target PPI (protein-protein interaction) network was built using STRING and the core targets were analyzed using GO with KEGG. The main active compounds against the targets were confirmed by molecular docking analysis. Based on the results, 158 compounds were identified in *A. muricata*, and the human body was found to absorb 56. It was discovered that 20 compounds were associated with cholesterol disease. The highest degree of the disease pathway of target compounds disease was annomuricin, XDH, myocardial ischemia, and metabolic pathways, respectively. The PPI showed GAPDH (glyceraldehyde-3-phosphate dehydrogenase) protein also has the highest degree. BP, CC, MF, and KEEG enrichments that play important roles are the response to drugs, plasma membranes, protein binding, and metabolic pathways. The molecular docking experiment confirmed the correlation between ligands and receptors (quercetin-XDH, coclaurine-ADRB3, fisetin, and robinetin-XDH) with binding energies of –9.3; –8.9; and –8.8 kcal $mol^{-1}$, respectively. The interactions between ligands and receptors are hydrogen, alkyl, Pi-alkyl, Pi-sigma, and van der Waals bonds. It was discovered that *A. muricata* provided therapeutic effects, involving multi-compounds, multi-targets, multi-diseases, and multi-pathways as well as deep insight into the pathogenesis of hyperlipidemia. This can be used to design new drugs and develop novel therapies to treat hyperlipidemia.

Keywords: AMPK signaling; antihyperlipidemia; herbal medicine; phytochemicals; soursop

ABSTRAK

Durian belanda (*Annona muricata* L.) adalah salah satu tumbuhan yang mempunyai kesan antihiperlipidemik, tetapi mekanisme tindakan asasnya masih tidak diketahui. Penyelidikan sebelumnya menggunakan TCMSP, KNApSAcK, ETCM, SwissTargetPrediction, SuperPred, CTD dan TTD untuk mengenal pasti sasaran potensi durian belanda sebagai antihiperlipidemik. Oleh itu, kajian ini bertujuan untuk meneroka sebatian aktif durian belanda dan menunjukkan mekanismenya terhadap hiperlipidemia melalui rangkaian farmakologi dan dok molekul. OB dan sifat keserupaan dadah bagi sebatian daripada *A. muricata* telah disaring berdasarkan parameter Lipinski's Ro5 (Lipinski's Rule of Five). Selepas itu, rangkaian sebatian-sasaran-penyakit-laluan dibina menggunakan Cytoscape. Rangkaian sasaran PPI (interaksi protein-protein) dibina menggunakan STRING dan sasaran teras dianalisis menggunakan GO dengan KEGG. Sebatian aktif utama terhadap sasaran telah disahkan oleh analisis dok molekul. Berdasarkan keputusan, 158 sebatian dikenal pasti dalam *A. muricata* dan tubuh manusia didapati menyerap 56. Didapati bahawa 20 sebatian dikaitkan dengan penyakit kolesterol. Peratusan tertinggi laluan penyakit, penyakit sebatian sasaran

masing-masing ialah annomuricin, XDH, iskemia miokardium dan laluan metabolik. PPI menunjukkan protein GAPDH (glyceraldehyde-3-phosphate dehydrogenase) juga mempunyai peratusan tertinggi. Pengayaan BP, CC, MF dan KEEG yang memainkan peranan penting ialah tindak balas terhadap ubat, membran plasma, pengikatan protein dan laluan metabolik. Uji kaji dok molekul mengesahkan korelasi antara ligan dan reseptor (quercetin-XDH, coclaurine-ADRB3, fisetin, dan robinetin-XDH) dengan tenaga mengikat masing-masing -9.3; –8.9; dan –8.8 kcal $mol^{-1.}$ *A. muricata* memberikan kesan terapeutik, melibatkan pelbagai sebatian, pelbagai sasaran, pelbagai penyakit dan pelbagai laluan serta pandangan mendalam tentang patogenesis hiperlipidemia. Ini boleh digunakan untuk mereka bentuk ubat baharu dan membangunkan terapi baru untuk merawat hiperlipidemia.

Kata kunci: Antihiperlipidemia; durian belanda; fitokimia; pengisyaratan AMPK; ubat herba

## Introduction

Hyperlipidemia is a risk factor for atherosclerosis, cardiovascular disease, stroke, and diabetes mellitus (Jiang et al. 2022; Nunes & Quintão 2022). It increases one or more cholesterols, phospholipids, or triglycerides, characterized by an elevation in total cholesterol, LDL (low-density lipoprotein), and TG (triglycerides) accompanied by a decrease in HDL (high-density lipoprotein) (Jing et al. 2022; Severino et al. 2020; Yao, Li & Zeng 2020). Hyperlipidemia can be treated with antihyperlipidemic drugs, but the use of synthetic drugs has more significant side effects than traditional ones (Obika et al. 2022).

In Indonesia, people in certain regions traditionally use soursop (*Annona muricata* L.) as an antihyperlipidemic. It was discovered that the roots, leaves, stem bark, and fruit pulp from plant can be used as antidiabetic and antioxidant (Agu & Okolie 2017; Handayani et al. 2022), anticancer (Gavamukulya et al. 2014), antiobesity, and alternative treatment for type 2 diabetes mellitus (Wang et al. 2021a). Furthermore, anti-inflammatory, smooth muscle relaxant, sedative, hypotensive, and antispasmodic effects are reported from the plant's leaves, barks, and roots (Moghadamtousi et al. 2015). Secondary metabolites that are contained in the leaves of *A. muricata* include alkaloids, terpenoids, saponins, and flavonoids. The previous study by Coria-Téllez et al. (2018) identified that alkaloid compounds, flavonoids, and tannins can reduce LDL cholesterol. The mechanism of active compounds in *A. muricata* such as pharmacological activities, interactions between compounds and target proteins, as well as disease pathways from the perspective of network pharmacology and molecular docking, is still unclear, specifically for antihyperlipidemic activity. Network analysis, bioinformatics, and molecular docking can be used to study the mechanism (Lu et al. 2022). For traditional medicine, several investigations showed that network pharmacology used in conjunction with molecular docking and simulation can effectively predict pharmacological mechanisms through multi-component and multi-target interactions (Fan et al. 2022; Liu et al. 2022). Network pharmacology analysis usually uses machine learning, graph mining, molecular docking, simulation modeling, and other techniques to analyze the relationships between compounds, target proteins, diseases, and pathways. These techniques were widely carried out in the search for active compounds from plant that have the potential for antihyperlipidemic (Wang et al. 2022a).

This study used network pharmacology to explore the underlying mechanisms and targets of the *A. muricata* compound for treating hyperlipidemia. Molecular docking was also used to validate correlations between the active compounds and potential target genes. The flowchart of network pharmacology and molecular docking technology employed is shown in Figure S1.

## Materials and Methods

### Data and tools

The main active components of *A. muricata* were mined from a literature review (Abdul Wahab et al. 2018; Gavamukulya et al. 2014; Gleye et al. 2000; Naik & Sellappan 2020; Rojas-Armas et al. 2022). The scientific name of herbs was used as the keyword to retrieve all compounds, while the secondary metabolites and types were determined. The duplication of compounds was eliminated during the construction of the database. Furthermore, online databases, namely KNApSAcK Family (http://www.knapsackfamily.com/KNApSAcK_Family/), TCMSP (traditional Chinese medicine systems pharmacology database and analysis platform) (http://lsp.nwsuaf.edu.cn/tcmsp.php) (Ru et al. 2014), and ETCM (The encyclopedia of traditional Chinese medicine)

(http://www.nrc.ac.cn:9090/ETCM/index.PHP/home/index/), were used. The active compounds were confirmed by the online databases, namely PubChem (https://pubchem.ncbi.nlm.nih.gov/), ChemSpider (http://www.chemspider.com/), Molbase (www.molbase.com), and SpectraBase (https://spectrabase.com/). The molecular structure of each active compound was confirmed using the online database and stored in *.pdb and SMILES formats. The chemical structures of the compounds were converted to pdb and SMILES format using MarvinSketch 19.6 (https://chemaxon.com/products/marvin) when the format was unavailable in the online database.

### CALCULATION AND PREDICTION OF ABSORPTION PARAMETERS

Lipinski's Ro5 was used for predicting absorption parameters, with MW less than 500, the number of hydrogen bond donors, namely hydrogen atoms attached to O and N, nOHNH was less than 5. Furthermore, the number of hydrogen bond acceptors, which were O and N, nON, were less than 10, and the lipid water partition coefficient (miLogP) was less than 5 (Lipinski 2004). Files from the online database and MarvinSketch 19.6 in SMILES format were analyzed using Molinspiration Cheminformatics (https://www.molinspiration.com/) and *.pdb formats using Lipinski Ro5 (http://www.scfbio-iitd.res.in/). The compounds that met the parameters were selected for further analysis.

### SCREENING AND PREDICTION OF POTENTIAL TARGETS

For each compound, the potential targets were predicted using SwissTargetPrediction (http://www.swisstargetprediction.ch/) (Gfeller et al. 2014) and the SuperPred website (http://prediction.charite.de/) by setting the attribute of *Homo sapiens*. By removing duplicate information, the Swiss Target and SuperPred prediction were used to predict *A. muricata* target proteins. The selected targets were applied to further analysis by referring to the TTD (therapeutic target database) (https://db.idrblab.org/ttd/) (Li et al. 2018) to obtain target protein-related diseases.

### SCREENING AND PREDICTION OF THE DISEASE PATHWAY

Disease targets were analyzed using the CTD (comparative toxicogenomics database) (http://ctdbase.org/) disease database. The identified diseases were integrated into the KEGG (Kyoto encyclopedia of genes and genomes) (https://www.genome.jp/kegg/) to obtain the most common disease pathways associated with the target genes. Subsequently, the target was identified with a p-value of 0.01 (Davis et al. 2019) to obtain the disease and its pathways.

### NETWORK PHARMACOLOGY CONSTRUCTION

Cytoscape ver. 3.8.2 (https://cytoscape.org/) software was used to construct the models, namely 1. multi-compounds–multi-targets, 2. multi-targets–multi-diseases, 3. multi-diseases–multi-pathways, 4. multi-compounds–targets–diseases–pathways, and 5. multi-compounds–diabetes gene targets–hyperlipidemia disease–hyperlipidemia pathways, and Merge were used to combine the two network models into the component–target–disease–pathway (C–T–D–P). The network analyzer function in the software was used to further analyze the network model's relations. Topology features were applied to evaluate network interactions, namely degree, betweenness, and closeness centrality. The nodes in different shapes and colors of the network represented active compounds, targets, diseases, and pathways, while the edges indicated their interaction. The degree refers to the number of nodes directly connected. The high degree values reflect the node's importance in the network, indicating that the node is more important. Furthermore, the active core compounds were screened, and the targets showing above-average values among the three parameters were selected based on degree values (Ye, Li & Hu 2021).

### CONSTRUCTION OF PROTEIN-PROTEIN INTERACTION (PPI) NETWORK

The PPI network was constructed by importing the candidate genes to the STRING, which is the search tool for the retrieval of interacting genes, ver. 11.0 (https://string-db.org) database (Szklarczyk et al. 2018), with the highest confidence of 0.9. It was applied to predict potential interactions and evaluate the overlap between target genes using a unique *Homo sapiens* database. In this study, the confidence score was employed to measure the likelihood of PPI. The higher the confidence score the protein sequence pair has, the more likely the pair will interact. The results obtained were analyzed using Cytoscape ver. 3.8.2 (Saito et al. 2012) and the PPI that underlies the mechanism of hyperlipidemia was obtained. The features were used to evaluate network interactions, namely degree, betweenness, and closeness centrality. The three parameters' highest value was used to determine the target protein.

### FUNCTIONAL ENRICHMENT ANALYSIS OF GO (GENE ONTOLOGY)

GO was analyzed using DAVID Bioinformatics Resources 6.8 server (https://david.ncifcrf.gov/home.jsp) (Sherman et al. 2022) and STRING ver. 11.0 (https://stringdb.org). SRplot (http://www.bioinformatics.com.cn/en) was used to process the data and visualize the enrichment results of GO, including BP (biological process), MF (molecular function), CC (cellular component), and KEGG.

### COMPONENT-TARGET MOLECULAR DOCKING

The analysis of molecular binding between the ligand and receptor was carried out to examine the binding mode and free energy, the type and distance of bonds, as well as amino acid residues. Subsequently, two-dimensional (2D) structures of ligands were extracted from the PubChem data bank (https://pubchem.ncbi.nlm.nih.gov/), and the receptors that match the target (specific to *Homo sapiens*) were obtained from RCSB PDB (protein data bank) (https://www.rscb.org/). This analysis used UCSF Chimera ver. 1.15 (https://www.cgl.ucsf.edu/chimera/) for ligand optimization (force field MMFF94 and algorithm Steepest Descent) and PyRx (https://pyrx.sourceforge.io/) equipped with AutoDock Vina to perform molecular docking. The conformation with the best affinity and lowest binding energy scores was selected as the final docking conformation and visualized by PyMOL ver. 2.3 (https://pymol.org/2/) and BIOVIA Discovery Studio 2019 (https://www.3dsbiovia.com). The hydrogen bonds and their binding sites were observed and analyzed. Finally, ligand-receptor interactions were displayed as 2D and 3D diagrams (Umar et al. 2022).

## RESULTS

### COLLECTION AND SCREENING OF CANDIDATE ACTIVE COMPOUNDS IN *A. muricata*

A total of 158 compounds were identified from *A. muricata*, while the main active components that qualified the absorption parameters by following Lipinski's Ro5 were 56 compounds, as shown in Table S1.

### TARGET PREDICTION

The compounds that met the parameters of Lipinski's Ro5 were further analyzed with SwissTargetPrediction. The results obtained were 560 targets, which were examined using the Therapeutic Target Database program to identify diseases related to the targets of each compound. The results were analyzed using CTD to determine the cholesterol disease pathway.

### NETWORK PHARMACOLOGY OF *A. muricata*

A pharmacological network was created to determine the relationship between compounds, targets, diseases, and pathways of *A. muricata* compounds that met the absorption parameters, as shown in Figure 1. The nodes and edges formed in the C–T–D–P component tissue were 425 and 1056, respectively. The target compounds and disease pathways with the highest grade values in the tissue were morin, fisetin, coronin, DRD2, asthma, and cytokine-cytokine receptor interactions, as presented in Tables S2-S5.

A pharmacological network devoted to cholesterol in form of a compound–target–disease–pathway in Figure 2 caused nodes and edges of 39 and 72, respectively. Meanwhile, only 20 of the 56 compounds in *A. muricata* were associated with cholesterol disease in this network. The pharmacological network of cholesterol disease with the highest degree of compound, target, disease, and pathway were anomurine, (+)-anomurine, anomurine and coclaurine, XDH (xanthine dehydrogenase), myocardial ischemia, and metabolic pathways, respectively.

The compounds anomurine, (+)-anomurine, anomurine, and coclaurine target two cholesterol diseases. The target proteins of the four compounds are ADRB2 (adrenergic receptor beta-2) and ADRB3 (adrenergic receptor beta-3), while the disease is based on the pharmacological network, namely hyperlipidemia and myocardial ischemia. One of the pathways for hyperlipidemia is the AMPK signaling pathway (5′ AMP-activated protein kinase), which involves genes that play a role in hyperlipidemia, as shown in Figure 3. The core targets that correlate with hyperlipidemia include ADRA1A, PP2A, HMGR, IGF1R, P13K, and PPARγ.

### PROTEIN-PROTEIN INTERACTION (PPI) NETWORK

Figure 4 shows that the PPI network consists of 164 nodes and 464 edges. The results of the interaction network analysis of GAPDH protein (glyceraldehyde-3-phosphate dehydrogenase) had the highest degree, betweenness, and closeness centrality of 63, 0.0721, and 0.5776, respectively, as illustrated in TABLE S6.

### GO AND KEGG ENRICHMENT ANALYZE

The analysis of GO on target genes used parameters for BP, CC, MF, and KEEG disease pathways, and was

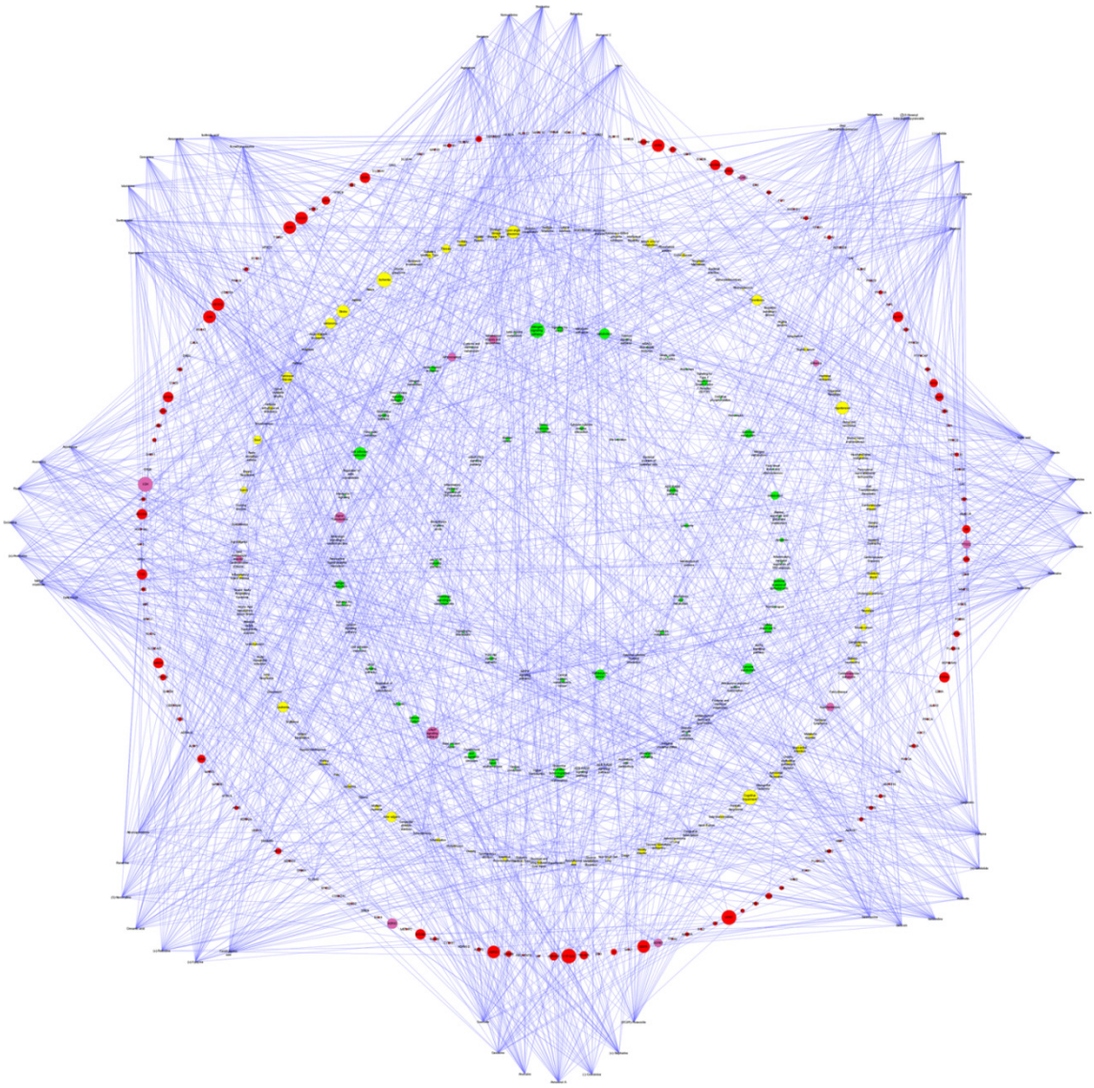

FIGURE 1. Network pharmacology of multi-compounds–multi-targets–multi-diseases–multi-pathways (C–T–D–P). The larger nodes represent more important hub nodes. Nodes in the outer ring represent the compounds. Node (inner ring) color indicates target (red), disease (yellow), and pathway (green). The purple nodes indicate each specific target, disease, and pathway associated with hyperlipidemia

evaluated with the Bonferroni method and p-value < 0.01. Figure 5 shows the results of the top 15 GO (BP, CC, and MF) and top 25 (KEGG) in –logP value, as well as the green color in the KEGG pathway, which indicates a more significant enrichment of GO terms. Furthermore, BP, CC, MF, and the KEGG played the most roles, namely response to drugs, plasma membrane, protein binding, and metabolic pathway, with enrichment scores of 18.50, 57.10, 63.10, and 35, respectively.

## RESULTS OF COMPOUNDS-TARGET MOLECULE DOCKING

Compounds and targets of pharmacological networks associated with cholesterol disease were analyzed using molecular docking. During this process, four ligands with the lowest bond affinity (negative value) were obtained, namely quercetin, coclaurine, fisetin, and robinetin with values –9.3, –8.9, –8.8, and –8.8 kcal $mol^{-1}$, respectively. The residues and amino acid bonds that occur in the

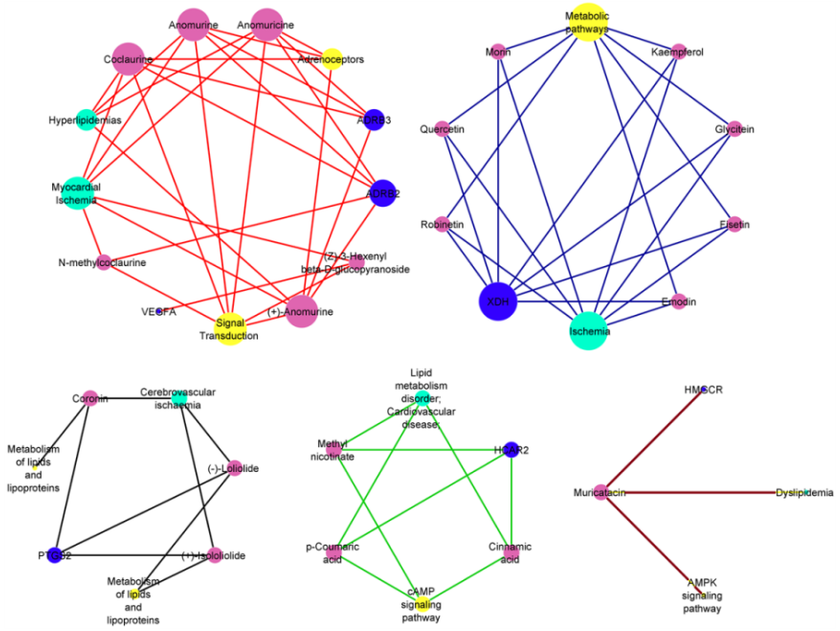


FIGURE 2. Networks between compounds-target-disease-pathways for hyperlipidemia. The larger the circle size, the more interaction there is between nodes. Node color indicates pink (compound), blue (target), green (disease), and yellow (pathway)

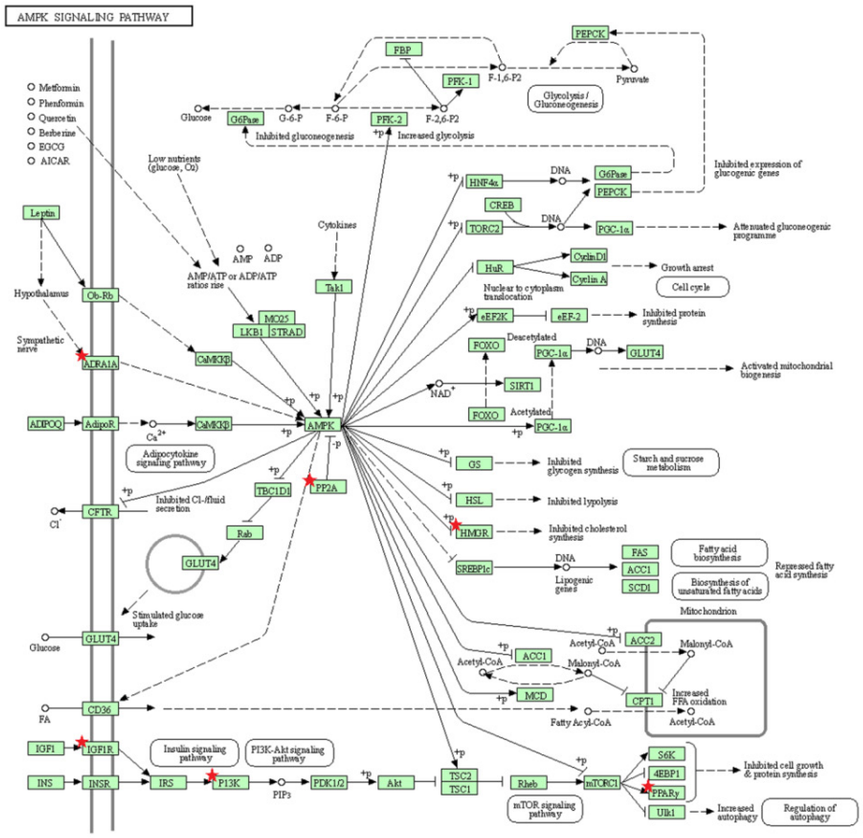


FIGURE 3. AMPK signaling pathway mechanism in hyperlipidemia. Red asterisks represent core targets

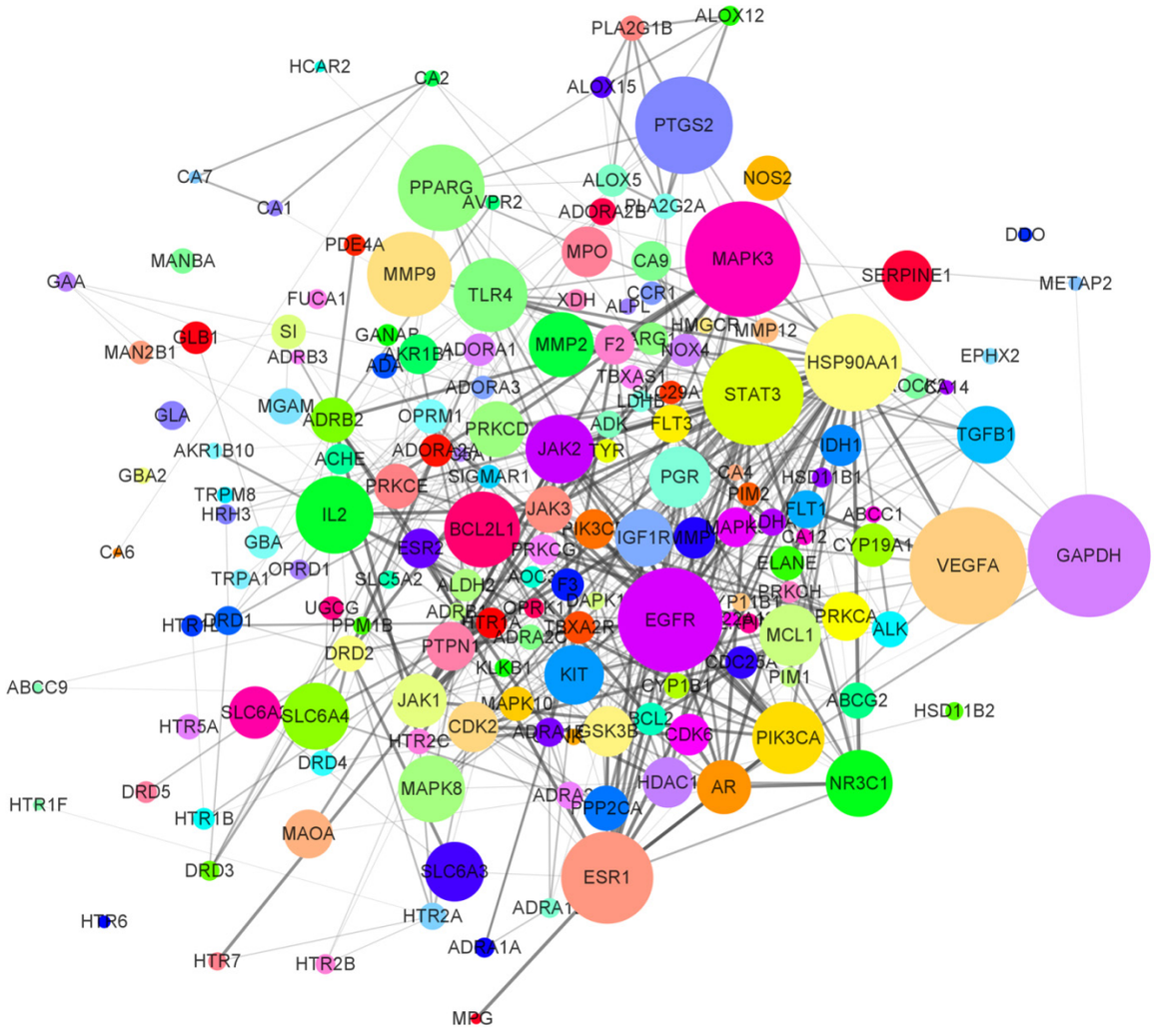


FIGURE 4. Network of protein-protein interaction. The size of the circle indicates the number of proteins correlated with the target

interaction between the four ligands and their receptors are summarized in Figure 6.

Quercetin-XDH binds through hydrogen bonds with Ser289, coclaurine-ADRB3 through Tyr59, Arg150, and Leu318, fisetin-XDH through Ile326 and Met329, as well as robinetin-XDH via Leu228, Glu295, and Ile326. The results of molecular docking, including residue, binding energy, and bond distance of the four ligands and their receptors are summarized in Table S7, and the 2D and 3D views in Figure S2.

## DISCUSSION

The combination of network pharmacology and molecular docking has been applied in this study. Both methods can be used to examine the mechanism of action of *A. muricata* compounds in treating hyperlipidemia. Exploration of herbal medicines for the management of complex diseases such as hyperlipidemia using network pharmacology is a well-accepted approach.

The development of new drug candidates is often constrained by their lack of ADME (absorption, distribution, metabolism, and excretion) properties. This high-cost nature makes the drug development process more difficult. Although ADME is an essential process in drug discovery and development, OB (oral bioavailability) is the most significant pharmacokinetic

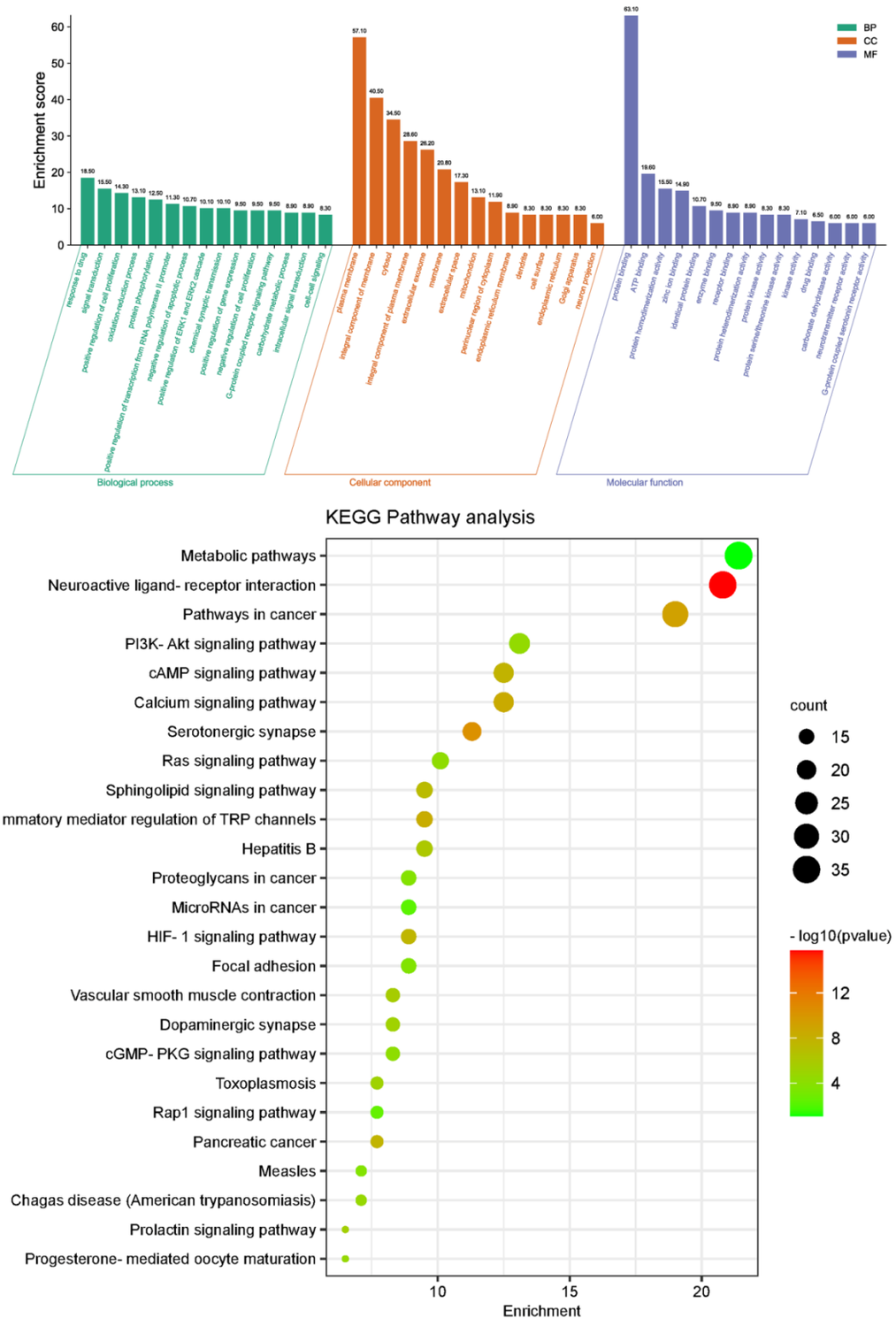


FIGURE 5. Enrichments analysis of the candidate target of *A. muricata* by gene ontology (GO) against hyperlipidemia. Biological process (BP) (green chart), cellular component (CC) (brown chart), molecular function (MF) (blue chart), KEGG pathway (bubble chart)

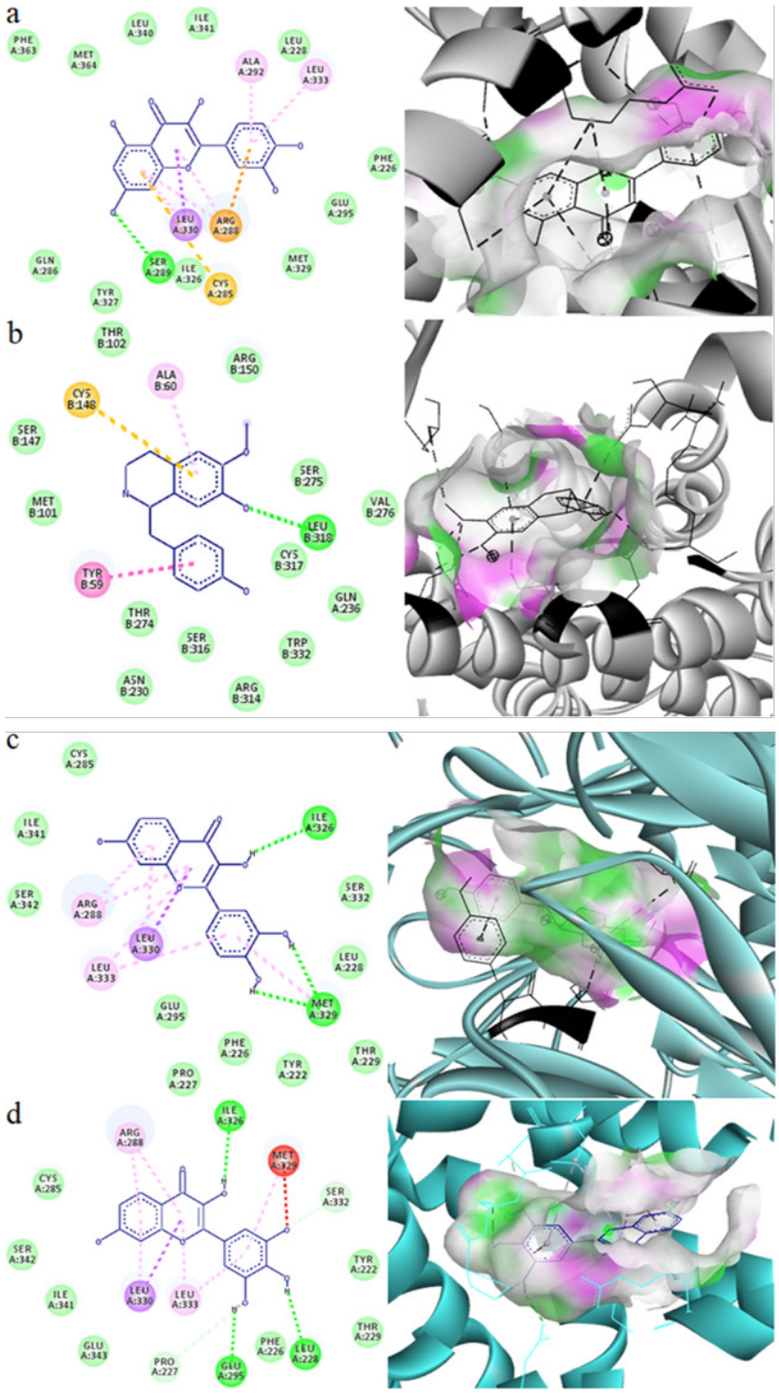


FIGURE 6. The represented results for the action mode of active compounds with target protein using molecular docking. Ligands and receptors on the protein's active site (2D and 3D view). Quercetin with target XDH (a), coclaurine and ADRB3 (b), fisetin (c) and robinetin (d) with XDH

parameter. This study identified 158 compounds from *A. muricata*, but only 56 were considered eligible. Some compounds with poor solubility and permeability cause absorption problems (Lipinski 2004). One of the parameters of an excellent medicinal compound for oral use is the ability to be adequately absorbed by the body. Furthermore, Lipinski's Ro5 parameters such as MW (molecular weight) (500), miLog P (5), nON (hydrogen bond acceptors) (5), and NOHNH (hydrogen donors) (10) can be used to determine the absorption of natural compounds (Ibrahim et al. 2021).

The results of the pharmacological network analysis showed that the compounds with the highest degree belonged to the alkaloid group, namely anomuricine, (+)-anomurine, anomurine, and coclaurine. This compound belongs to the class of alkaloids (Abdul Wahab et al. 2018; Coria-Téllez et al. 2018; Pieme et al. 2014; Ragasa et al. 2012). A previous report showed that alkaloids have cholesterol-lowering activity with a mechanism of action for inhibiting dietary cholesterol uptake and HMG-CoA (hydroxy-3-methyl-glutaryl coenzyme A) reductase activity (Maharjan et al. 2022).

Alkaloid compounds interact with ADRB3 and ADRB2, with G-protein coupled receptors as the target. ADRB3 induces WAT (white adipose tissue) lipolysis and increases BAT's (brown adipose tissue) thermogenesis (Pinto, Festuccia & Magdalon 2022). ADRB3 mutations in white adipose cells can slow lipolysis, causing lipid retention in adiposity and significantly increasing leptin and dyslipidemia (Daghestani et al. 2018). ADRB2 remotes the mobilization of stored triglycerides and ADIPOQ (adiponectin), secreted by adipose tissue stimulates autophagy by inhibiting mTORC1 and promoting the activation of AMPK (Tripathi, Srivastava & Tripathi 2018). Moreover, AMPK signaling plays a crucial role in regulating cellular energy metabolism as shown in Figure 3. It is an essential metabolic sensor that regulates the body's energy balance (van der Vaart, Boon & Houtkooper 2021). An AMPK signaling molecule is highly correlated with the activation of cholesterol signaling-related molecules such as HMGCR (3-hydroxy-3-methylglutaryl-CoA reductase), FDFT1 (farnesyl-diphosphate farnesyltransferase 1), and LSS (lanosterol synthase) (Xu et al. 2022)PI3K (phosphoinositide 3-kinases) (Li et al. 2022a), PP2A (protein phosphatase 2A) (Ke et al. 2022), IGF1R (insulin-like growth factor 1 receptor) (Wang et al. 2022b), and PPAR (peroxisome proliferatoractivated receptor) (Berghoff, Spieth & Saher 2022).

Based on the PPI network, GAPDH has the highest degree, betweenness, and closeness centrality, indicating that the protein has the largest correlation to target PPI (Wang et al. 2022b). GAPDH is a glycolytic enzyme that catalyzes glyceraldehyde 3-phosphate to 1,3-diphosphoglycerate and increases glycolysis, where glucose is converted into pyruvic acid. Increased ROS (reactive oxygen species) and ischemia (atherosclerosis) by GAPDH can cause damage to mitochondria (Qvit et al. 2016). Ischemia often occurs due to atherosclerosis, a condition where cholesterol plaques form on the walls of arteries due to risk factors for diseases such as hypercholesterolemia, diabetes, and hypertension (Jebari-Benslaiman et al. 2022).

Response to the drug (BP), plasma membrane (CC), and protein binding (MF) had the highest scores on GO analysis. The three GO are most likely to underlie the antihyperlipidemic mechanism of soursop active compounds. Furthermore, drug response has a relationship that can affect the therapeutic effect. The reaction catalyzed by human HMG-CoA reductase targets antihyperlipidemic drugs (statins) to lower serum cholesterol levels. HMG-CoA reductase inhibitors are agents with healthy blood cholesterol and lipid-lowering effects that are used to prevent primary and secondary atherosclerosis. The enzyme HMG-CoA reductase catalyzes the conversion of HMG-CoA to mevalonate. This four-electron oxidoreduction is a rate-limiting step in synthesizing cholesterol and other isoprenoids (Li et al. 2022b). The plasma membrane also facilitates intracellular cholesterol transport, controls cellular cholesterol balance, and influences transcriptional regulation (Islam, Hlushchenko & Pfisterer 2022). Since protein binding is associated with biological responses, changes can cause a significant difference in biological responses. According to Ghaleb et al. (2022), binding proteins on the endoplasmic reticulum cause downregulation of LDL receptors, leading to hypercholesterolemia. Metabolic pathways are related to lipid metabolism and hypercholesterolemia diseases such as triglycerides, fatty acids, cholesterol esters, and phospholipids (Wang et al. 2021b).

Jin et al. (2021) stated that the lower the affinity (bond energy), the higher the bond strength between the ligand and the target protein. This indicated that the compound has a more stable bound to the receptor, while quercetin, coclaurine, fisetin, and robinetin bind to receptors through hydrogen bonds. The formation of hydrogen bonds minimizes the energy of the complex

between the molecule-receptor, thereby making it stable (Yu et al. 2021).

The mechanism of quercetin is inhibiting low-density lipoprotein oxidation by suppressing myeloperoxidase-catalyzed oxidation and plays an anti-inflammatory, antioxidant, and lipid-lowering role in AFLD by decreasing serum and hepatic NF-B, p65, COX-2, and IL-6. The decreased activated AMPK (Lin et al. 2022) which contributes to the pathogenesis of liver steatosis. Lipophagy-related Rab7 has been presumed as a crucial regulator in the progression of alcohol liver disease despite elusive mechanisms. More importantly, whether or not hepatoprotective quercetin targets Rab7-associated lipophagy disorder is unknown. Herein, alcoholic fatty liver induced by chronic-plus-single-binge ethanol feeding to male C57BL/6J mice was manifested by hampering autophagosomes formation with lipid droplets and fusion with lysosomes compared with the normal control, which was normalized partially by quercetin. The GST-RILP pulldown assay of Rab7 indicated an improved GTP-Rab7 as the quercetin treatment for ethanol-feeding mice. HepG2 cells transfected with CYP2E1 showed similar lipophagy dysfunction when exposed to ethanol, which was blocked when cells were transfected with siRNA-Rab7 in advance. Ethanol-induced steatosis and autophagic flux disruption were aggravated by the Rab7-specific inhibitor CID1067700 while alleviated by transfecting with the Rab7Wt plasmid, which was visualized by immunofluorescence co-localization analysis and mCherry-GFP-LC3 transfection. Furthermore, TBC1D5, a Rab GTPase-activating protein for the subsequent normal circulation of Rab7, was downregulated after alcohol administration but regained by quercetin. Rab7 circulation retarded by ethanol and corrected by quercetin was further shown by fluorescence recovery after photobleaching (FRAP, involved the PI3K signaling pathway (Wang et al. 2022b). Several studies showed that quercetin exerts anti-adipogenic effects in 3 T3-L1 cells by inhibiting the adipocyte-specific transcription factors PPAR-γ as well as C/EBPα and activating the AMPK signaling pathways (Chang, Lee & Chiang 2012). Coclaurine exhibited significant effects in hyperlipidemia (Yang et al. 2022), while Fisetin, a bioflavonoid possesses anti-inflammatory, antilipidemic, and anticancer properties. It was discovered that fisetin can also ameliorate and reduce oxLDL-induced upregulation of SREBP-1, thereby expressing its downstream lipid synthesis genes HMGCR and FAS, which inhibit ROS induced NLRP3 inflammasome activation (Varghese et al. 2021). Robinetin correlated with high antioxidant activity (Sari et al. 2021), known free radicals, specifically ROS, which is another critical mechanism involved in atherosclerosis development and progression (Mollazadeh et al. 2018).

## Conclusions

In this study, 56 compounds of *A. muricata* met the criteria for drug absorption parameters and pharmacological tissue, while 20 were associated with cholesterol disease. Coclaurine, anomuricine, (+)-anomurine, and anomurine compounds have the most targets, with ADRB2 and ADRB3 target proteins in hyperlipidemia and myocardial ischemia. BP, CC, MF, and KEEG have the most significant roles, namely response to drugs, plasma membranes, protein binding, and metabolic pathways. The molecular bonds of quercetin with XDH (3osi), coclaurine with ADRB3 (7dh5), fisetin, and robinetin with XDH (3osi) have binding energies of –9.3, –8.9, and –8.8 kcal $mol^{-1}$, respectively. This shows a holistic view of the potential pharmacological and molecular mechanisms of *A. muricata* as an antihyperlipidemic agent. The results provided new methods for investigating other traditional medicine compounds. However, limitations of this study include the use of computerized methods. Secondly, with the combination of network pharmacology and molecular docking, the therapeutic mechanism of active compounds from *A. muricata* is not fully understood. A comprehensive understanding depends on the expected development of multi-disciplines. Thirdly, the results need to be further verified by experiments.

## References

Abdul Wahab, S.M., Jantan, I., Haque, Md.A. & Arshad, L. 2018. Exploring the leaves of *Annona muricata* L. as a source of potential anti-inflammatory and anticancer agents. *Frontiers in Pharmacology* 9: 661.

Agu, K.C. & Okolie, P.N. 2017. Proximate composition, phytochemical analysis, and *in vitro* antioxidant potentials of extracts of *Annona muricata* (Soursop). *Food Science & Nutrition* 5(5): 1029-1036.

Berghoff, S.A., Spieth, L. & Saher, G. 2022. Local cholesterol metabolism orchestrates remyelination. *Trends in Neurosciences* 45(4): 272-283.

Cárdenas, C., Torres-Vargas, J.A., Cárdenas-Valdivia, A., Jurado, N., Quesada, A.R., García-Caballero, M., Martínez-Poveda, B. & Medina, M.Á. 2021. Non-targeted metabolomics characterization of *Annona muricata* leaf extracts with anti-angiogenic activity. *Biomedicine & Pharmacotherapy* 144: 112263.

Chang, Y.C., Lee, T.S. & Chiang, A.N. 2012. Quercetin enhances ABCA1 expression and cholesterol efflux through a p38-dependent pathway in macrophages. *Journal of Lipid Research* 53(9): 1840-1850.

Coria-Téllez, A.V., Montalvo-Gónzalez, E., Yahia, E.M. & Obledo-Vázquez, E.N. 2018. *Annona muricata*: A comprehensive review on its traditional medicinal uses, phytochemicals, pharmacological activities, mechanisms of action and toxicity. *Arabian Journal of Chemistry* 11(5): 662-691.

Daghestani, M., Daghestani, M., Daghistani, M., Eldali, A., Hassan, Z.K., Elamin, M.H. & Warsy, A. 2018. ADRB3 polymorphism rs4994 (Trp64Arg) associates significantly with bodyweight elevation and dyslipidaemias in Saudis but not rs1801253 (Arg389Gly) polymorphism in ARDB1. *Lipids in Health and Disease* 17(1): 58.

Davis, A.P., Grondin, C.J., Johnson, R.J., Sciaky, D., McMorran, R., Wiegers, J., Wiegers, T.C. & Mattingly, C.J. 2019. The comparative toxicogenomics database: Update 2019. *Nucleic Acids Research* 47(D1): D948-D954.

Fan, L., Feng, S., Wang, T., Ding, X., An, X., Wang, Z., Zhou, K., Wang, M., Zhai, X. & Li, Y. 2022. Chemical composition and therapeutic mechanism of Xuanbai Chengqi Decoction in the treatment of COVID-19 by network pharmacology, molecular docking and molecular dynamic analysis. *Molecular Diversity* 27(1): 81-102.

Gavamukulya, Y., Abou-Elella, F., Wamunyokoli, F. & AEl-Shemy, H. 2014. Phytochemical screening, anti-oxidant activity and *in vitro* anticancer potential of ethanolic and water leaves extracts of *Annona muricata* (Graviola). *Asian Pacific Journal of Tropical Medicine* 7: S355-S363.

Gfeller, D., Grosdidier, A., Wirth, M., Daina, A., Michielin, O. & Zoete, V. 2014. SwissTargetPrediction: A web server for target prediction of bioactive small molecules. *Nucleic Acids Research* 42(W1): W32-W38.

Ghaleb, Y., Elbitar, S., Philippi, A., El Khoury, P., Azar, Y., Andrianirina, M., Loste, A., Abou-Khalil, Y., Nicolas, G., Le Borgne, M., Moulin, P., Di-Filippo, M., Charrière, S., Farnier, M., Yelnick, C., Carreau, V., Ferrières, J., Lecerf, J.M., Derksen, A., Bernard, G., Gauthier, M.S., Coulombe, B., Lütjohann, D., Fin, B., Boland, A., Olaso, R., Deleuze, J.F., Rabès, J.P., Boileau, C., Abifadel, M. & Varret, M. 2022. Whole exome/genome sequencing joint analysis of a family with oligogenic familial hypercholesterolemia. *Metabolites* 12(3): 262.

Gleye, C., Raynaud, S., Fourneau, C., Laurens, A., Laprévote, O., Serani, L., Fournet, A. & Hocquemiller, R. 2000. Cohibins C and D, two important metabolites in the biogenesis of acetogenins from *Annona muricata* and *Annona nutans*. *Journal of Natural Products* 63(9): 1192-1196.

Handayani, S.I., Sari, M.I.P., Sardjana, M.S., Kusmardi, K., Nurbaya, S., Rosmalena, R., Sinaga, E. & Prasasty, V.D. 2022. Ameliorative effects of *Annona muricata* leaf ethanol extract on renal morphology of alloxan-induced mice. *Applied Sciences* 12(18): 9141.

Ibrahim, M.A.A., Abdeljawaad, K.A.A., Abdelrahman, A.H.M. & Hegazy, M.E.F. 2021. Natural-like products as potential SARS-CoV-2 Mpro inhibitors: *in-silico* drug discovery. *Journal of Biomolecular Structure and Dynamics* 39(15): 5722-5734.

Islam, M.M., Hlushchenko, I. & Pfisterer, S.G. 2022. Low-density lipoprotein internalization, degradation and receptor recycling along membrane contact sites. *Frontiers in Cell and Developmental Biology* 24(10): 826379.

Jebari-Benslaiman, S., Galicia-García, U., Larrea-Sebal, A., Olaetxea, J.R., Alloza, I., Vandenbroeck, K., Benito-Vicente, A. & Martín, C. 2022. Pathophysiology of atherosclerosis. *International Journal of Molecular Sciences* 23(6): 3346.

Jiang, L., Xiong, Y., Tu, Y., Zhang, W., Zhang, Q., Nie, P., Yan, X., Liu, H., Liu, R. & Xu, G. 2022. Elucidation of the transport mechanism of puerarin and gastrodin and their interaction on the absorption in a Caco-2 cell monolayer model. *Molecules* 27(4): 1230.

Jin, J., Chen, B., Zhan, X., Zhou, Z., Liu, H. & Dong, Y. 2021. Network pharmacology and molecular docking study on the mechanism of colorectal cancer treatment using Xiao-Chai-Hu-Tang. *PLoS ONE* 16(6): e0252508.

Jing, Y.S., Ma, Y.F., Pan, F.B., Li, M.S., Zheng, Y.G., Wu, L.F. & Zhang, D.S. 2022. An insight into antihyperlipidemic effects of polysaccharides from natural resources. *Molecules* 27(6): 1903.

Ke, W., Zhou, Y., Lai, Y., Long, S., Fang, L. & Xiao, S. 2022. Porcine reproductive and respiratory syndrome virus nsp4 positively regulates cellular cholesterol to inhibit type I interferon production. *Redox Biology* 49: 102207.

Li, D., Zhang, J. & Liu, Q. 2022a. Brain cell type-specific cholesterol metabolism and implications for learning and memory. *Trends in Neurosciences* 45(5): 401-414.

Li, J., Zhu, F., Xu, W. & Che, P. 2022b. Therapeutic properties of isoliquiritigenin with molecular modeling studies: investigation of anti-pancreatic acinar cell tumor and HMG-CoA reductase inhibitor activity for treatment of hypercholesterolemia. *Archives of Medical Science*. https://doi.org/10.5114/aoms/145448

Li, Y.H., Yu, C.Y., Li, X.X., Zhang, P., Tang, J., Yang, Q., Fu, T., Zhang, X., Cui, X., Tu, G., Zhang, Y., Li, S., Yang, F., Sun, Q., Qin, C., Zeng, X., Chen, Z., Chen, Y.Z. & Zhu, F. 2018. Therapeutic target database update 2018: Enriched resource for facilitating bench-to-clinic research of targeted therapeutics. *Nucleic Acids Research* 46(Database issue): D1121-D1127.

Lin, H., Guo, X., Liu, J., Liu, P., Mei, G., Li, H., Li, D., Chen, H., Chen, L., Zhao, Y., Jiang, C., Yu, Y., Liu, W. & Yao, P. 2022. Improving lipophagy by restoring Rab7 cycle: Protective effects of quercetin on ethanol-induced liver steatosis. *Nutrients* 14(3): 658.

Lipinski, C.A. 2004. Lead and drug like compounds: The rule of five revolution. *Drug Discovery Today Technologies* 1(4): 337-341.

Liu, C., Fan, F., Zhong, L., Su, J., Zhang, Y. & Tu, Y. 2022. Elucidating the material basis and potential mechanisms of Ershiwuwei Lvxue Pill acting on rheumatoid arthritis by UPLC-Q-TOF/MS and network pharmacology. *PLoS ONE* 17(2): e0262469.

Lu, S., Tang, L., Zhou, L., Lai, Y., Liu, L. & Duan, Y. 2022. Study on the multitarget mechanism and active compounds of essential oil from *Artemisia argyi* treating pressure injuries based on network pharmacology. *Evidence-Based Complementary and Alternative Medicine* 2022: e1019289.

Maharjan, B., Payne, D.T., Ferrarese, I., Giovanna Lupo, M., Kumar Shrestha, L., Hill, J.P., Ariga, K., Rossi, I., Sharan Shrestha, S., Panighel, G., Lal (Swagat) Shrestha, R., Sut, S., Ferri, N. & Dall'Acqua, S. 2022. Evaluation of the effects of natural isoquinoline alkaloids on low density lipoprotein receptor (LDLR) and proprotein convertase subtilisin/kexin type 9 (PCSK9) in hepatocytes, as new potential hypocholesterolemic agents. *Bioorganic Chemistry* 121: 105686.

Moghadamtousi, S.Z., Fadaeinasab, M., Nikzad, S., Mohan, G., Ali, H.M. & Kadir, H.A. 2015. *Annona muricata* (Annonaceae): A review of its traditional uses, isolated acetogenins and biological activities. *International Journal of Molecular Sciences* 16(7): 15625-15658.

Mollazadeh, H., Carbone, F., Montecucco, F., Pirro, M. & Sahebkar, A. 2018. Oxidative burden in familial hypercholesterolemia. *Journal of Cellular Physiology* 233(8): 5716-5725.

Naik, A.V. & Sellappan, K. 2020. Chromatographic fingerprint of essential oils in plant organs of *Annona muricata* L. (Annonaceae) using HPTLC. *Analytical Chemistry Letters* 10(2): 214-226.

Nunes, V.S., da Silva Ferreira, G. & Quintão, E.C.R. 2022. Cholesterol metabolism in aging simultaneously altered in liver and nervous system. *Aging* 14(3): 1549-1561.

Obika, P., Beamon, J., Ali, S., Kakar, N., Analla, A., Moudden, R.E., Shihadeh, L., Patel, S., Hudson, B., Khan, F., Puglisi-Weening, M., Basist, P., Ahmad, S. & Shahid, M. 2022. 6 - Herbal medicines for the treatment of metabolic syndrome. In. *Herbal Medicines*, edited by Sarwat, M. & Siddique, H. Massachusetts: Academic Press. hlm. 139-191.

Pieme, C.A., Kumar, S.G., Dongmo, M.S., Moukette, B.M., Boyoum, F.F., Ngogang, J.Y. & Saxena, A.K. 2014. Antiproliferative activity and induction of apoptosis by *Annona muricata* (Annonaceae) extract on human cancer cells. *BMC Complementary and Alternative Medicine* 14(1): 516.

Pinto, Y.O., Festuccia, W.T.L. & Magdalon, J. 2022. The involvement of the adrenergic nervous system in activating human brown adipose tissue and browning. *Hormones* 21(2): 195-208.

Qvit, N., Joshi, A.U., Cunningham, A.D., Ferreira, J.C.B. & Mochly-Rosen, D. 2016. Glyceraldehyde-3-phosphate dehydrogenase (GAPDH) protein-protein interaction inhibitor reveals a non-catalytic role for GAPDH oligomerization in cell death. *Journal of Biological Chemistry* 291(26): 13608-13621.

Ragasa, C.Y., Soriano, G., Torres, O.B., Don, M.J. & Shen, C.C. 2012. Acetogenins from *Annona muricata*. *Pharmacognosy Journal* 4(32): 32-37.

Rojas-Armas, J.P., Arroyo-Acevedo, J.L., Palomino-Pacheco, M., Ortiz-Sánchez, J.M., Calva, J., Justil-Guerrero, H.J., Castro-Luna, A., Ramos-Cevallos, N., Cieza-Macedo, E.C. & Herrera-Calderon, O. 2022. Phytochemical constituents and ameliorative effect of the essential oil from *Annona muricata* L. leaves in a murine model of breast cancer. *Molecules* 27(6): 1818.

Ru, J., Li, P., Wang, J., Zhou, W., Li, B., Huang, C., Li, P., Guo, Z., Tao, W., Yang, Y., Xu, X., Li, Y., Wang, Y. & Yang, L. 2014. TCMSP: A database of systems pharmacology for drug discovery from herbal medicines. *Journal of Cheminformatics* 6(1): 13.

Saito, R., Smoot, M.E., Ono, K., Ruscheinski, J., Wang, P.L., Lotia, S., Pico, A.R., Bader, G.D. & Ideker, T. 2012. A travel guide to Cytoscape plugins. *Nature Methods* 9(11): 1069-1076.

Sari, R.K., Prayogo, Y.H., Sari, R.A.L., Asidah, N., Rafi, M., Wientarsih, I. & Darmawan, W. 2021. *Intsia bijuga* heartwood extract and its phytosome as tyrosinase inhibitor, antioxidant, and sun protector. *Forests* 12(12): 1792.

Severino, P., D'Amato, A., Pucci, M., Infusino, F., Adamo, F., Birtolo, L.I., Netti, L., Montefusco, G., Chimenti, C., Lavalle, C., Maestrini, V., Mancone, M., Chilian, W.M. & Fedele, F. 2020. Ischemic heart disease pathophysiology paradigms overview: From plaque activation to microvascular dysfunction. *International Journal of Molecular Sciences* 21(21): 8118.

Sherman, B.T., Hao, M., Qiu, J., Jiao, X., Baseler, M.W., Lane, H.C., Imamichi, T. & Chang, W. 2022. DAVID: A web server for functional enrichment analysis and functional annotation of gene lists (2021 update). *Nucleic Acids Research* 50(W1): W216-W221.

Szklarczyk, D., Gable, A., Lyon, D., Junge, A., Wyder, S., Huerta-Cepas, J., Simonovic, M., Doncheva, N., Morris, J., Bork, P., Jensen, L. & von Mering, C. 2018. STRING v11: protein-protein association networks with increased coverage, supporting functional discovery in genome-wide experimental datasets. *Nucleic Acids Research* 47(D1): D607-D613.

Tripathi, S., Srivastava, S. & Tripathi, Y.B. 2018. Obesity and its complications: Role of autophagy. *International Journal of Pharmaceutical Sciences and Research* 9(8): 3100-3113.

Umar, A.H., Ratnadewi, D., Rafi, M., Sulistyaningsih, Y.C., Hamim, H. & Kusuma, W.A. 2022. Drug candidates and potential targets of *Curculigo* spp. compounds for treating diabetes mellitus based on network pharmacology, molecular docking and molecular dynamics simulation. *Journal of Biomolecular Structure and Dynamics*. doi: 10.1080/07391102.2022.2135597

van der Vaart, J.I., Boon, M.R. & Houtkooper, R.H. 2021. The role of AMPK signaling in brown adipose tissue activation. *Cells* 10(5): 1122.

Varghese, J.F., Patel, R., Singh, M. & Yadav, U.C.S. 2021. Fisetin prevents oxidized low-density lipoprotein–induced macrophage foam cell formation. *Journal of Cardiovascular Pharmacology* 78(5): e729-e737.

Wang, B., Wang, H., Li, Y. & Song, L. 2022a. Lipid metabolism within the bone micro-environment is closely associated with bone metabolism in physiological and pathophysiological stages. *Lipids in Health and Disease* 21(1): 5.

Wang, H., Wang, H., Zhang, J., Luo, J., Peng, C., Tong, X. & Chen, X. 2022b. Molecular mechanism of Crataegi Folium and Alisma Rhizoma in the treatment of dyslipidemia based on network pharmacology and molecular docking. *Evidence-Based Complementary and Alternative Medicine* 2022: e4891370.

Wang, F.X., Zhu, N., Zhou, F. & Lin, D.X. 2021a. Natural aporphine alkaloids with potential to impact metabolic syndrome. *Molecules* 26(20): 6117.

Wang, Q., Du, L., Hong, J., Chen, Z., Liu, H., Li, S., Xiao, X. & Yan, S. 2021b. Molecular mechanism underlying the hypolipidemic effect of Shanmei Capsule based on network pharmacology and molecular docking. *Technology and Health Care* 29(S1): 239-256.

Xu, X.Y., Choi, H.S., Park, S.Y., Kim, J.K., Seo, K.H., Kim, H. & Kim, Y.J. 2022. *Hibiscus syriacus* L. cultivated in callus culture exerts cytotoxicity in colorectal cancer via Notch signaling-mediated cholesterol biosynthesis suppression. *Phytomedicine* 95: 153870.

Yang, J., Zhang, Y., Jiang, L., Li, C., Sun, Z., Zhang, Y., Lin, T., Jiang, Y. & Liu, B. 2022. A triple combination strategy of UHPLC-MSn, hypolipidemic activity and transcriptome sequencing to unveil the hypolipidemic mechanism of *Nelumbo nucifera* alkaloids. *Journal of Ethnopharmacology* 282: 114608.

Yao, Y.S., Li, T.D. & Zeng, Z.H. 2020. Mechanisms underlying direct actions of hyperlipidemia on myocardium: An updated review. *Lipids in Health and Disease* 19(1): 23.

Ye, J., Li, L. & Hu, Z. 2021. Exploring the molecular mechanism of action of Yinchen Wuling powder for the treatment of hyperlipidemia, using network pharmacology, molecular docking, and molecular dynamics simulation. *BioMed Research International* 2021: e9965906.

Yu, J., Yuan, H., Bao, L. & Si, L. 2021. Interaction between piperine and genes associated with sciatica and its mechanism based on molecular docking technology and network pharmacology. *Molecular Diversity* 25(1): 233-248.

*Corresponding author; email: ahuhalim76@yahoo.com

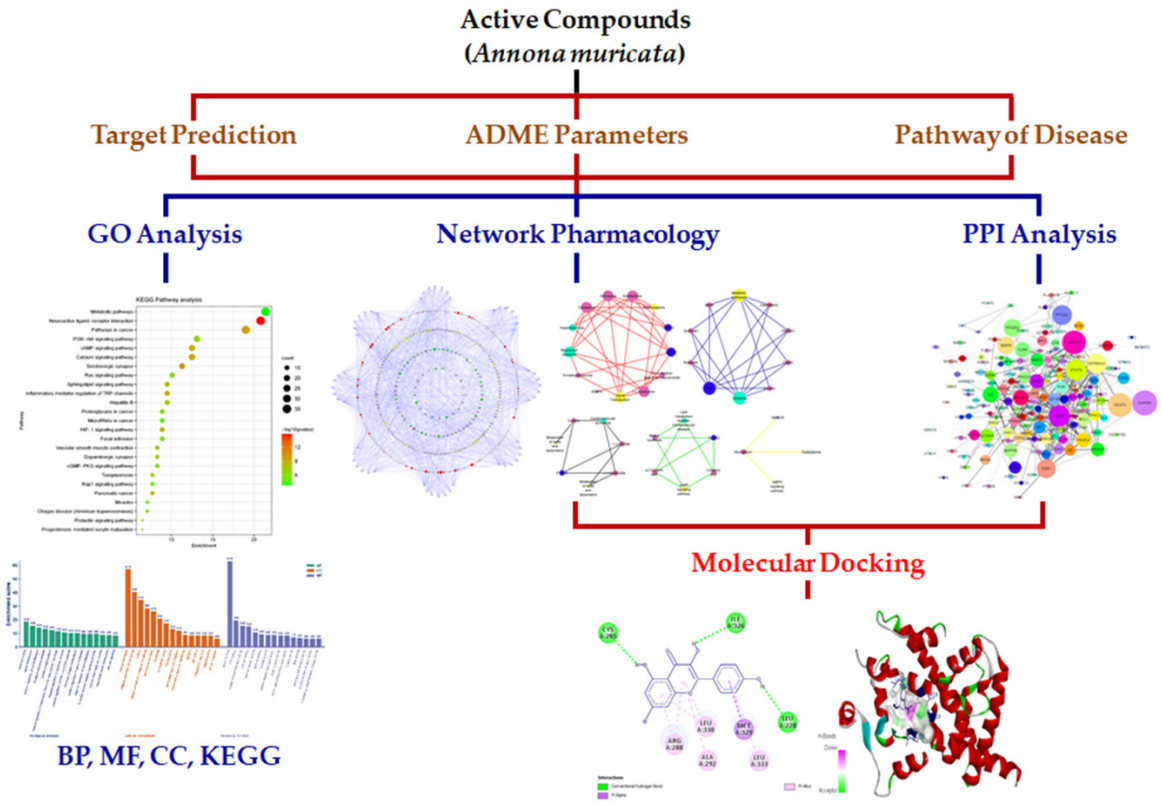


FIGURE S1. Workflow for network pharmacology and molecular docking technology

TABLE S1. *A. muricata* compound and absorption parameters

| No | Compound | Absorption parameters | | | | Result |
|---|---|---|---|---|---|---|
| | | miLogP (≤5) | nOHNH (≤5) | nON (≤10) | MW (≤500) | |
| 1 | p-Coumaric acid | 1.43 | 2 | 3 | 164.16 | ✓ |
| 2 | Epoxymurin-A | 9.91 | 0 | 3 | 530.88 | × |
| 3 | Squamocin | 8.80 | 3 | 7 | 622.93 | × |
| 4 | Anonaine | 3.25 | 1 | 3 | 265.31 | ✓ |
| 5 | (+)-Reticuline | 2.38 | 2 | 5 | 329.40 | ✓ |
| 6 | (+)-Xylopine | 3.29 | 1 | 4 | 295.34 | ✓ |
| 7 | Coronin | 2.29 | 0 | 5 | 260.25 | ✓ |
| 8 | Gallic acid | 0.59 | 4 | 5 | 170.12 | ✓ |
| 9 | 3-O-Caffeoylquinic acid | -0.45 | 6 | 9 | 354.31 | × |
| 10 | Kaempferol | 2.17 | 4 | 6 | 286.24 | ✓ |
| 11 | Quercetin | 1.68 | 5 | 7 | 302.24 | ✓ |
| 12 | kaempferol 3-O-robinobioside | -0.57 | 9 | 15 | 594.52 | × |
| 13 | Nicotiflorin | -0.57 | 9 | 15 | 594.52 | × |
| 14 | Quercetin-3-O-glucoside | -0.36 | 8 | 12 | 464.38 | × |
| 15 | Rutin | -1.06 | 10 | 16 | 610.52 | × |
| 16 | (-)-Loliolide | 1.84 | 1 | 3 | 196.25 | ✓ |
| 17 | (+)-Isololiolide | 1.84 | 1 | 3 | 196.25 | ✓ |

| | | | | | | |
|---|---|---|---|---|---|---|
| 18 | Asimilobine | 2.90 | 2 | 3 | 267.33 | ✓ |
| 19 | (-)-Coreximine | 1.94 | 2 | 5 | 327.38 | ✓ |
| 20 | (+)-Stepharine | 1.66 | 1 | 4 | 297.35 | ✓ |
| 21 | Isolaureline | 3.53 | 0 | 4 | 309.37 | ✓ |
| 22 | Coclaurine | 2.31 | 3 | 4 | 285.34 | ✓ |
| 23 | Argentinine | 3.95 | 1 | 3 | 295.38 | ✓ |
| 24 | (S)-Norcorydine | 2.75 | 2 | 5 | 327.38 | ✓ |
| 25 | Nornuciferine | 3.21 | 1 | 3 | 281.36 | ✓ |
| 26 | (6S,9R)-Roseoside | -0.19 | 5 | 8 | 386.44 | ✓ |
| 27 | (Z)-3-Hexenyl beta-D-glucopyranoside | -0.36 | 4 | 6 | 262.30 | ✓ |
| 28 | Citroside A | -0.74 | 5 | 8 | 386.44 | ✓ |
| 29 | Neochlorogenic acid | -0.45 | 6 | 9 | 354.31 | × |
| 30 | Turpinionoside A | -0.12 | 6 | 8 | 390.47 | × |
| 31 | Sabadelin | 9.91 | 0 | 3 | 530.88 | × |
| 32 | Annonacin A | 8.41 | 4 | 7 | 596.89 | × |
| 33 | Donhexocin | 7.39 | 6 | 8 | 614.90 | × |
| 34 | Murihexocin C | 5.73 | 6 | 9 | 628.89 | × |
| 35 | Annomontacin | 8.92 | 4 | 7 | 624.94 | × |
| 36 | Annonacin | 8.41 | 4 | 7 | 596.89 | × |
| 37 | cis-Annomontacin | 8.92 | 4 | 7 | 624.94 | × |
| 38 | Annomuricatin B | -1.10 | 10 | 18 | 739.83 | × |
| 39 | Annonacinone | 8.28 | 3 | 7 | 594.87 | × |
| 40 | Annopentocin A | 7.12 | 5 | 8 | 612.89 | × |
| 41 | Annopentocin B | 7.12 | 5 | 8 | 612.89 | × |
| 42 | Annopentocin C | 7.12 | 5 | 8 | 612.89 | × |
| 43 | cis-Annonacin | 8.41 | 4 | 7 | 596.89 | × |
| 44 | cis-Goniothalamicin | 8.41 | 4 | 7 | 596.89 | × |
| 45 | Cohibin A | 9.74 | 2 | 4 | 548.89 | × |
| 46 | Cohibin B | 9.74 | 2 | 4 | 548.89 | × |
| 47 | Diepomuricanin A | 9.73 | 0 | 4 | 546.88 | × |
| 48 | Epomusenin A | 10.05 | 0 | 3 | 558.93 | × |
| 49 | Epomusenin B | 10.05 | 0 | 3 | 558.93 | × |
| 50 | Epoxymurin B | 9.91 | 0 | 3 | 530.88 | × |
| 51 | Gigantetrocin A | 8.41 | 4 | 7 | 596.89 | × |
| 52 | Gigantetronenin | 8.71 | 4 | 7 | 622.93 | × |
| 53 | Goniothalamicin | 8.41 | 4 | 7 | 596.89 | × |
| 54 | Isoannonacin | 7.10 | 3 | 7 | 596.89 | × |
| 55 | Isoannonacin-10-one | 6.91 | 2 | 7 | 594.87 | × |
| 56 | Javoricin | 8.41 | 4 | 7 | 596.89 | × |
| 57 | Longifolicin | 9.06 | 3 | 6 | 580.89 | × |
| 58 | Methyl nicotinate | 0.53 | 0 | 3 | 137.14 | × |
| 59 | Montecristin | 9.82 | 2 | 4 | 574.93 | × |
| 60 | Muricatetrocin A | 8.41 | 4 | 7 | 596.89 | × |
| 61 | Muricatetrocin B | 8.41 | 4 | 7 | 596.89 | × |
| 62 | Muricatin B | 7.57 | 5 | 8 | 612.89 | × |
| 63 | Muridienin 3 | 10.19 | 0 | 2 | 542.93 | × |
| 64 | Murihexocin A | 5.73 | 6 | 9 | 628.89 | × |

| | | | | | | |
|---|---|---|---|---|---|---|
| 65 | Murihexocin B | 5.73 | 6 | 9 | 628.89 | × |
| 66 | Neoannonin | 9.05 | 2 | 6 | 578.88 | × |
| 67 | Xylomaticin | 8.92 | 4 | 7 | 624.94 | × |
| 68 | Annocatalin | 8.41 | 4 | 7 | 596.89 | × |
| 69 | cis-Corossolone | 8.99 | 2 | 6 | 578.88 | × |
| 70 | Muricin H | 9.06 | 3 | 6 | 580.89 | × |
| 71 | Muricin I | 9.23 | 3 | 6 | 606.93 | × |
| 72 | Muricin A | 8.41 | 4 | 7 | 596.89 | × |
| 73 | Muricin B | 8.41 | 4 | 7 | 596.89 | × |
| 74 | Muricin C | 8.41 | 4 | 7 | 596.89 | × |
| 75 | Muricin D | 7.49 | 4 | 7 | 568.84 | × |
| 76 | Muricin E | 7.49 | 4 | 7 | 568.84 | × |
| 77 | Muricin F | 8.01 | 4 | 7 | 594.87 | × |
| 78 | Muricin G | 8.02 | 4 | 7 | 594.87 | × |
| 79 | Cohibin C | 9.90 | 2 | 4 | 576.95 | × |
| 80 | Cohibin D | 9.90 | 2 | 4 | 576.95 | × |
| 81 | Annoreticuin-9-one | 8.28 | 3 | 7 | 594.87 | × |
| 82 | Chatenaytrienin 1 | 10.01 | 0 | 2 | 512.86 | × |
| 83 | Chatenaytrienin 2 | 10.01 | 0 | 2 | 512.86 | × |
| 84 | Chatenaytrienin 3 | 10.14 | 0 | 2 | 540.92 | × |
| 85 | Chatenaytrienin 4 | 10.14 | 0 | 2 | 540.92 | × |
| 86 | Rollimusin | 7.62 | 4 | 8 | 638.93 | × |
| 87 | cis-Reticulatacin-10-one | 9.31 | 2 | 6 | 606.93 | × |
| 88 | cis-Solamin | 9.51 | 2 | 5 | 564.89 | × |
| 89 | cis-Uvariamicin I | 9.71 | 2 | 5 | 592.95 | × |
| 90 | cis-Uvariamicin IV | 9.71 | 2 | 5 | 592.95 | × |
| 91 | Muricapentocin | 6.88 | 5 | 8 | 612.89 | × |
| 92 | Purpurenin | 7.62 | 4 | 8 | 638.93 | × |
| 93 | Muricatacin | 4.50 | 1 | 3 | 284.44 | ✓ |
| 94 | Anomuricine | 3.06 | 2 | 5 | 329.40 | ✓ |
| 95 | (+)-Anomurine | 3.34 | 1 | 5 | 343.42 | ✓ |
| 96 | Annoionol A | 1.70 | 3 | 3 | 230.35 | ✓ |
| 97 | Annoionoside | -0.97 | 7 | 9 | 406.47 | × |
| 98 | Annomuricin E | 7.35 | 5 | 8 | 612.89 | × |
| 99 | Annonamine | -0.83 | 1 | 3 | 296.39 | × |
| 100 | Arianacin | 8.41 | 4 | 7 | 596.89 | × |
| 101 | Atherosperminine | 4.26 | 0 | 3 | 309.41 | ✓ |
| 102 | Epomuricenin B | 9.91 | 0 | 3 | 530.88 | × |
| 103 | Corepoxylone | 9.34 | 0 | 5 | 560.86 | × |
| 104 | cis-annonacin-10-one | 7.11 | 3 | 7 | 594.87 | × |
| 105 | Blumenol C | 2.48 | 1 | 2 | 210.32 | ✓ |
| 106 | Gigantetrocin | 8.41 | 4 | 7 | 596.89 | × |
| 107 | Muricadienin | 10.07 | 0 | 2 | 514.88 | × |
| 108 | Muricatenol | 9.30 | 4 | 6 | 608.95 | × |
| 109 | Muridienin 3 | 10.19 | 0 | 2 | 542.93 | × |
| 110 | Muridienin 4 | 10.19 | 0 | 2 | 542.93 | × |
| 111 | 15-Palmitoylsolamin | 10.50 | 1 | 6 | 803.31 | × |
| 112 | 15-Oleoylsolamin | 10.54 | 1 | 6 | 829.35 | × |

| | | | | | | |
|---|---|---|---|---|---|---|
| 113 | Robustocin | 9.38 | 1 | 5 | 562.88 | × |
| 114 | Annonaine | 3.25 | 1 | 3 | 265.31 | ✓ |
| 115 | Anomurine | 3.34 | 1 | 5 | 343.42 | ✓ |
| 116 | Casuarine | -3.17 | 5 | 6 | 205.21 | ✓ |
| 117 | Coreximine | 1.94 | 2 | 5 | 327.38 | ✓ |
| 118 | DMJ (Deoxymannojirimycin) | -2.40 | 5 | 5 | 163.17 | ✓ |
| 119 | Isoboldine | 2.49 | 2 | 5 | 327.38 | ✓ |
| 120 | Liriodenine | 3.30 | 0 | 4 | 275.26 | ✓ |
| 121 | N-methylcoclaurine | 2.56 | 2 | 4 | 299.37 | ✓ |
| 122 | Muricinine | 2.48 | 3 | 5 | 313.35 | ✓ |
| 123 | Remerine | 3.50 | 0 | 3 | 279.34 | ✓ |
| 124 | Reticuline | 2.38 | 2 | 5 | 329.40 | ✓ |
| 125 | Stepharine | 1.66 | 1 | 4 | 297.35 | ✓ |
| 126 | Swainsonine | -1.34 | 3 | 4 | 173.21 | ✓ |
| 127 | Xylopine | 3.29 | 1 | 4 | 295.34 | ✓ |
| 128 | Emodin | 3.01 | 3 | 5 | 270.24 | ✓ |
| 129 | Chlorogenic acid | -0.45 | 6 | 9 | 354.31 | × |
| 130 | Dicaffeoylquinic acid | 1.21 | 7 | 12 | 516.46 | × |
| 131 | Feruloylquinic acid | -0.14 | 5 | 9 | 368.34 | ✓ |
| 132 | Cinnamic acid | 1.91 | 1 | 2 | 148.16 | ✓ |
| 133 | Apigenin-6-C-glucoside | 0.52 | 7 | 10 | 432.38 | × |
| 134 | Daidzein | 2.56 | 2 | 4 | 254.24 | ✓ |
| 135 | Fisetin | 1.97 | 4 | 6 | 286.24 | ✓ |
| 136 | Gallocatechin | 1.08 | 6 | 7 | 306.27 | × |
| 137 | Genistein | 2.27 | 3 | 5 | 270.24 | ✓ |
| 138 | Glycitein | 2.38 | 2 | 5 | 284.27 | ✓ |
| 139 | Homoorientin | 0.03 | 8 | 11 | 448.38 | × |
| 140 | Isoferulic acid | 1.25 | 2 | 4 | 194.19 | ✓ |
| 141 | Kaempferol 3-O-rutinoside | -0.57 | 9 | 15 | 594.52 | × |
| 142 | Luteolin 3′7-di-O-glucoside | -1.83 | 10 | 16 | 610.52 | × |
| 143 | Morin | 1.88 | 5 | 7 | 302.24 | ✓ |
| 144 | Myricetin | 1.39 | 6 | 8 | 318.24 | × |
| 145 | Quercetin 3-O-glucoside | -0.36 | 8 | 12 | 464.38 | × |
| 146 | Quercetin 3-Oneohesperidoside | -1.06 | 10 | 16 | 610.52 | × |
| 147 | Robinetin | 1.68 | 5 | 7 | 302.24 | ✓ |
| 148 | Tangeretin | 3.78 | 0 | 7 | 372.37 | ✓ |
| 149 | Vitexin | 0.52 | 7 | 10 | 432.38 | ✓ |
| 150 | Caffeic acid | 0.94 | 3 | 4 | 180.16 | ✓ |
| 151 | Gentisic acid | 1.37 | 3 | 4 | 154.12 | ✓ |
| 152 | Diepomuricanin B | 9.73 | 0 | 4 | 546.88 | × |
| 153 | Annoglaxin | 6.70 | 4 | 8 | 610.87 | × |
| 154 | Annohexocin | 5.73 | 6 | 9 | 628.89 | × |
| 155 | Annomuricin A | 7.35 | 5 | 8 | 612.89 | × |
| 156 | Corossolin | 9.06 | 3 | 6 | 580.89 | × |
| 157 | Annopentocin C | 7.12 | 5 | 8 | 612.89 | × |
| 158 | Corossolone | 8.99 | 2 | 6 | 578.88 | × |

Note: ✓ = qualified, × = not qualified

TABLE S2. Betweenness centrality, closeness centrality, and degree of compounds

| No | Name | Betweenness centrality | Closeness centrality | Degree |
|---|---|---|---|---|
| 1 | p-Coumaric acid | 0.034892097 | 0.36637931 | 30 |
| 2 | Anonaine | 0.008801786 | 0.353577371 | 24 |
| 3 | (+)-Reticuline | 0.014299228 | 0.341091493 | 25 |
| 4 | (+)-Xylopine | 0.010418774 | 0.342190016 | 27 |
| 5 | Coronin | 0.079710764 | 0.358347386 | 30 |
| 6 | Gallic acid | 0.038732665 | 0.30227596 | 29 |
| 7 | Kaempferol | 0.029008477 | 0.35475793 | 29 |
| 8 | Quercetin | 0.03578424 | 0.365748709 | 29 |
| 9 | (-)-Loliolide | 0.030585147 | 0.326923077 | 24 |
| 10 | (+)-Isololiolide | 0.030585147 | 0.326923077 | 24 |
| 11 | Asimilobine | 0.010551658 | 0.358952703 | 25 |
| 12 | (-)-Coreximine | 0.011620587 | 0.351239669 | 25 |
| 13 | (+)-Stepharine | 0.043923983 | 0.313884786 | 29 |
| 14 | Isolaureline | 0.025282923 | 0.346655791 | 26 |
| 15 | Coclaurine | 0.013379154 | 0.352990033 | 27 |
| 16 | Argentinine | 0.026437044 | 0.346091205 | 25 |
| 17 | (S)-Norcorydine | 0.007904255 | 0.346091205 | 25 |
| 18 | Nornuciferine | 0.013093161 | 0.346655791 | 26 |
| 19 | (6S,9R)-Roseoside | 0.047730059 | 0.331513261 | 27 |
| 20 | (Z)-3-Hexenyl beta-D-glucopyranoside | 0.054880088 | 0.334119497 | 27 |
| 21 | Citroside A | 0.035457824 | 0.336234177 | 29 |
| 22 | Methyl nicotinate | 0.050437472 | 0.361394558 | 29 |
| 23 | Muricatacin | 0.087083252 | 0.307971014 | 28 |
| 24 | Anomuricine | 0.016857417 | 0.357744108 | 28 |
| 25 | (+)-Anomurine | 0.016238306 | 0.353577371 | 28 |
| 26 | Annoionol A | 0.042973403 | 0.315281899 | 30 |
| 27 | Annonamine | 0.013165109 | 0.346655791 | 26 |
| 28 | Atherosperminine | 0.00966975 | 0.340544872 | 24 |
| 29 | Blumenol C | 0.051661084 | 0.352404643 | 29 |
| 30 | Annonaine | 0.009052953 | 0.353577371 | 24 |
| 31 | Anomurine | 0.016857417 | 0.357744108 | 28 |
| 32 | Casuarine | 0.045626759 | 0.359560068 | 26 |
| 33 | Coreximine | 0.011620587 | 0.351239669 | 25 |
| 34 | DMJ (Deoxymannojirimycin) | 0.033335336 | 0.328438949 | 23 |
| 35 | Isoboldine | 0.010323133 | 0.358952703 | 25 |
| 36 | Liriodenine | 0.070717324 | 0.328438949 | 27 |
| 37 | N-methylcoclaurine | 0.011212004 | 0.356543624 | 26 |
| 38 | Muricinine | 0.007986528 | 0.346655791 | 26 |
| 39 | Remerine | 0.005613653 | 0.324427481 | 26 |
| 40 | Reticuline | 0.010008757 | 0.351821192 | 23 |
| 41 | Stepharine | 0.043923983 | 0.313884786 | 29 |
| 42 | Swainsonine | 0.034960183 | 0.329968944 | 26 |
| 43 | Xylopine | 0.009376627 | 0.342190016 | 27 |

| | | | | |
|---|---|---|---|---|
| 44 | Emodin | 0.049208969 | 0.352404643 | 27 |
| 45 | Feruloylquinic acid | 0.046048729 | 0.347790507 | 29 |
| 46 | Cinnamic acid | 0.025251299 | 0.332550861 | 28 |
| 47 | Daidzein | 0.026894829 | 0.353577371 | 27 |
| 48 | Genistein | 0.020785486 | 0.352404643 | 25 |
| 49 | Glycitein | 0.022896283 | 0.342190016 | 27 |
| 50 | Isoferulic acid | 0.029127108 | 0.360780985 | 28 |
| 51 | Morin | 0.049329588 | 0.343851133 | 30 |
| 52 | Robinetin | 0.027601314 | 0.365120275 | 28 |
| 53 | Tangeretin | 0.05422869 | 0.349506579 | 27 |
| 54 | Caffeic acid | 0.035556314 | 0.341091493 | 27 |
| 55 | Gentisic acid | 0.03519748 | 0.301846591 | 28 |
| 56 | Fisetin | 0.06314154 | 0.337301587 | 30 |

TABLE S3. Betweenness centrality, closeness centrality, and degree of the target

| No | Name | Betweenness centrality | Closeness centrality | Degree |
|---|---|---|---|---|
| 1 | AKR1B1 | 0.003419483 | 0.299717913 | 8 |
| 2 | CA2 | 0.010064459 | 0.32003012 | 12 |
| 3 | PTPN1 | 0.005232201 | 0.289115646 | 5 |
| 4 | TLR4 | 0.001030997 | 0.281084656 | 3 |
| 5 | CA1 | 0.005424507 | 0.306637807 | 10 |
| 6 | MMP9 | 3.10E+10 | 0.282204515 | 4 |
| 7 | ALOX5 | 0.00176057 | 0.294729542 | 5 |
| 8 | CA9 | 0.00750802 | 0.306637807 | 9 |
| 9 | HSD11B1 | 0 | 0.268308081 | 1 |
| 10 | HCAR2 | 1.44E+12 | 0.276692708 | 3 |
| 11 | DRD2 | 0.002700798 | 0.292297111 | 23 |
| 12 | HTR2A | 0.002702629 | 0.293103448 | 16 |
| 13 | SLC6A4 | 0.002350435 | 0.285234899 | 9 |
| 14 | HTR2B | 4.56E+12 | 0.281456954 | 12 |
| 15 | HTR2C | 7.09E+11 | 0.284090909 | 9 |
| 16 | HTR1D | 5.04E+10 | 0.274547804 | 6 |
| 17 | DRD3 | 4.22E+12 | 0.282579787 | 12 |
| 18 | HTR1B | 5.52E+10 | 0.271045918 | 5 |
| 19 | DRD5 | 2.27E+11 | 0.278141361 | 8 |
| 20 | DRD1 | 0.001685171 | 0.289509537 | 20 |
| 21 | ADRA1A | 7.32E+11 | 0.28638814 | 13 |
| 22 | HTR1A | 3.22E+12 | 0.280343008 | 9 |
| 23 | SIGMAR1 | 0.015027855 | 0.309766764 | 15 |
| 24 | SLC6A3 | 0.001881118 | 0.293508287 | 14 |
| 25 | DRD4 | 3.48E+11 | 0.282204515 | 11 |
| 26 | ADRA1D | 1.69E+12 | 0.279605263 | 8 |
| 27 | ADRA1B | 1.67E+11 | 0.263320942 | 4 |
| 28 | HTR7 | 6.23E+10 | 0.274193548 | 7 |
| 29 | CCR1 | 0.001668414 | 0.272785623 | 2 |
| 30 | PIK3CA | 0 | 0.263975155 | 1 |

| | | | | |
|---|---|---|---|---|
| 31 | HSP90AA1 | 0 | 0.263975155 | 1 |
| 32 | PTGS2 | 0.002155619 | 0.283711615 | 4 |
| 33 | PIK3CB | 0 | 0.263975155 | 1 |
| 34 | NOS2 | 0.00400527 | 0.292297111 | 4 |
| 35 | ALPL | 0 | 0.263975155 | 1 |
| 36 | ADORA2B | 0 | 0.263975155 | 1 |
| 37 | FLT1 | 0 | 0.263975155 | 1 |
| 38 | IGF1R | 4.57E+11 | 0.279605263 | 3 |
| 39 | ALK | 0 | 0.232240437 | 1 |
| 40 | SERPINE1 | 0 | 0.232240437 | 1 |
| 41 | CA12 | 0.002850776 | 0.299295775 | 8 |
| 42 | CA14 | 3.86E+12 | 0.279237845 | 4 |
| 43 | BCL2L1 | 0 | 0.232240437 | 1 |
| 44 | CA4 | 0.001959702 | 0.29432133 | 6 |
| 45 | NOX4 | 1.69E+12 | 0.278141361 | 4 |
| 46 | XDH | 0.002523969 | 0.295549374 | 7 |
| 47 | TYR | 0.002266947 | 0.287162162 | 5 |
| 48 | MAOA | 4.51E+12 | 0.284471218 | 5 |
| 49 | ALOX5 | 0 | 0.262022195 | 1 |
| 50 | ACHE | 8.83E+09 | 0.267969735 | 2 |
| 51 | ABCC1 | 2.80E+11 | 0.278505898 | 3 |
| 52 | AVPR2 | 1.16E+11 | 0.270700637 | 2 |
| 53 | CYP19A1 | 0.004454341 | 0.297619048 | 7 |
| 54 | EGFR | 0.002264381 | 0.290300546 | 6 |
| 55 | F2 | 1.56E+12 | 0.2763329 | 2 |
| 56 | PPARG | 4.62E+09 | 0.246806039 | 2 |
| 57 | ABCC9 | 4.62E+09 | 0.246806039 | 2 |
| 58 | PLA2G1B | 4.62E+09 | 0.246806039 | 2 |
| 59 | AR | 0.001459478 | 0.282579787 | 4 |
| 60 | CYP11B1 | 4.62E+09 | 0.246806039 | 2 |
| 61 | PGR | 4.62E+09 | 0.246806039 | 2 |
| 62 | PPP2CA | 4.62E+09 | 0.246806039 | 2 |
| 63 | HTR5A | 8.92E+09 | 0.270356234 | 4 |
| 64 | HTR6 | 4.67E+10 | 0.274547804 | 6 |
| 65 | F3 | 1.25E+11 | 0.267969735 | 3 |
| 66 | HTR1F | 1.59E+10 | 0.23957159 | 2 |
| 67 | MPO | 1.59E+10 | 0.23957159 | 2 |
| 68 | ROCK2 | 0 | 0.239032621 | 1 |
| 69 | PIM2 | 1.59E+10 | 0.23957159 | 2 |
| 70 | JAK3 | 1.59E+10 | 0.23957159 | 2 |
| 71 | JAK1 | 1.59E+10 | 0.23957159 | 2 |
| 72 | JAK2 | 1.59E+10 | 0.23957159 | 2 |
| 73 | PRKCE | 0.001420707 | 0.253579952 | 3 |
| 74 | ADRA2A | 0 | 0.257575758 | 1 |
| 75 | ADRA2C | 0 | 0.257575758 | 1 |
| 76 | ADRB2 | 1.92E+10 | 0.268308081 | 5 |
| 77 | ADRB1 | 1.07E+12 | 0.277777778 | 6 |
| 78 | TBXA2R | 8.85E+09 | 0.267632242 | 4 |

| | | | | |
|---|---|---|---|---|
| 79 | ADRB3 | 8.85E+09 | 0.267632242 | 4 |
| 80 | HRH3 | 0 | 0.257263923 | 1 |
| 81 | SLC6A2 | 1.27E+11 | 0.267295597 | 2 |
| 82 | AOC3 | 0 | 0.257263923 | 1 |
| 83 | OPRM1 | 5.79E+11 | 0.27997365 | 3 |
| 84 | PTPRCAP | 0 | 0.257575758 | 1 |
| 85 | SLC5A2 | 1.29E+11 | 0.262345679 | 2 |
| 86 | ADA | 1.29E+11 | 0.262345679 | 2 |
| 87 | ADORA2A | 0.002348895 | 0.293508287 | 5 |
| 88 | ADORA3 | 0.001018328 | 0.277053455 | 3 |
| 89 | HDAC1 | 0 | 0.24912075 | 1 |
| 90 | SLC5A1 | 0 | 0.24912075 | 1 |
| 91 | SLC29A1 | 0 | 0.24912075 | 1 |
| 92 | FUCA1 | 0.003199045 | 0.290697674 | 6 |
| 93 | PPM1B | 0 | 0.24912075 | 1 |
| 94 | STAT3 | 0 | 0.250589623 | 1 |
| 95 | IL2 | 1.75E+12 | 0.261377614 | 2 |
| 96 | ADORA1 | 0.002079948 | 0.29432133 | 5 |
| 97 | ADK | 0 | 0.250589623 | 1 |
| 98 | GAPDH | 0 | 0.250589623 | 1 |
| 99 | GAA | 8.36E+10 | 0.278871391 | 4 |
| 100 | VEGFA | 0 | 0.250589623 | 1 |
| 101 | EPHX2 | 0 | 0.251777251 | 1 |
| 102 | METAP2 | 0 | 0.251777251 | 1 |
| 103 | DDO | 0 | 0.265625 | 1 |
| 104 | TRPA1 | 0 | 0.265625 | 1 |
| 105 | PIM1 | 3.08E+12 | 0.275974026 | 2 |
| 106 | KLKB1 | 0 | 0.265625 | 1 |
| 107 | PRKCA | 0 | 0.235587583 | 1 |
| 108 | PDE4A | 0 | 0.235587583 | 1 |
| 109 | HMGCR | 0 | 0.235587583 | 1 |
| 110 | PRKCG | 0 | 0.235587583 | 1 |
| 111 | PRKCH | 0 | 0.235587583 | 1 |
| 112 | PRKCD | 0 | 0.235587583 | 1 |
| 113 | OPRK1 | 0 | 0.235587583 | 1 |
| 114 | TRPM8 | 0 | 0.239841986 | 1 |
| 115 | HSD11B1 | 3.09E+11 | 0.2763329 | 2 |
| 116 | ESR1 | 0.001036036 | 0.286002692 | 5 |
| 117 | ESR2 | 0.001879392 | 0.292699725 | 6 |
| 118 | CDC25A | 0 | 0.239841986 | 1 |
| 119 | HSD11B2 | 0 | 0.260736196 | 1 |
| 120 | NR3C1 | 0 | 0.260736196 | 1 |
| 121 | SERPINA6 | 0 | 0.260736196 | 1 |
| 122 | MAPK3 | 0 | 0.260736196 | 1 |
| 123 | MGAM | 0.001445826 | 0.282579787 | 5 |
| 124 | GANAB | 1.47E+12 | 0.268987342 | 3 |
| 125 | SI | 1.47E+12 | 0.268987342 | 3 |

| | | | | |
|---|---|---|---|---|
| 126 | MANBA | 5.88E+10 | 0.267632242 | 2 |
| 127 | GBA2 | 1.47E+12 | 0.268987342 | 3 |
| 128 | PLA2G2A | 0 | 0.264632628 | 1 |
| 129 | UGCG | 0 | 0.247380675 | 1 |
| 130 | GBA | 1.19E+11 | 0.249413146 | 2 |
| 131 | GLA | 0 | 0.247380675 | 1 |
| 132 | GLB1 | 1.19E+11 | 0.249413146 | 2 |
| 133 | IDH1 | 0 | 0.247380675 | 1 |
| 134 | GSK3B | 0 | 0.247380675 | 1 |
| 135 | MAPK8 | 0 | 0.247380675 | 1 |
| 136 | MAPK10 | 0 | 0.247380675 | 1 |
| 137 | MAPK9 | 0 | 0.247380675 | 1 |
| 138 | CDK2 | 4.70E+11 | 0.259146341 | 2 |
| 139 | TGFB1 | 0 | 0.247380675 | 1 |
| 140 | ROCK2 | 0 | 0.239032621 | 1 |
| 141 | MAN2B1 | 0 | 0.248247664 | 1 |
| 142 | CSNK2A1 | 0 | 0.260736196 | 1 |
| 143 | ELANE | 2.60E+12 | 0.275974026 | 2 |
| 144 | FNTA FNTB | 0 | 0.260736196 | 1 |
| 145 | MCL1 | 0 | 0.260736196 | 1 |
| 146 | BCL2 | 0 | 0.260736196 | 1 |
| 147 | MMP2 | 7.09E+10 | 0.272785623 | 2 |
| 148 | AKR1B10 | 0 | 0.258201701 | 1 |
| 149 | ALOX5 | 0 | 0.258201701 | 1 |
| 150 | MMP12 | 0 | 0.258201701 | 1 |
| 151 | CA5B | 1.55E+10 | 0.271392082 | 2 |
| 152 | ALDH2 | 0 | 0.261377614 | 1 |
| 153 | TBXAS1 | 7.01E+09 | 0.263647643 | 2 |
| 154 | CDK6 | 0 | 0.252375297 | 1 |
| 155 | ALOX15 | 0 | 0.252375297 | 1 |
| 156 | ALOX12 | 0 | 0.252375297 | 1 |
| 157 | ARG1 | 0 | 0.252375297 | 1 |
| 158 | CA5A | 0 | 0.265293383 | 1 |
| 159 | DAPK1 | 0 | 0.256024096 | 1 |
| 160 | MPG | 0 | 0.256024096 | 1 |
| 161 | SLC22A12 | 0 | 0.256024096 | 1 |
| 162 | FLT3 | 7.75E+09 | 0.274547804 | 2 |
| 163 | OPRD1 | 0 | 0.259146341 | 1 |
| 164 | ABCG2 | 0 | 0.259146341 | 1 |
| 165 | CYP1B1 | 0 | 0.259146341 | 1 |
| 166 | KIT | 0 | 0.259146341 | 1 |
| 167 | CA7 | 1.01E+12 | 0.266624843 | 2 |
| 168 | CA6 | 1.01E+12 | 0.266624843 | 2 |
| 169 | MMP1 | 0 | 0.254491018 | 1 |
| 170 | LDHA | 0 | 0.2319869 | 1 |
| 171 | LDHB | 0 | 0.2319869 | 1 |

TABLE S4. Betweenness centrality, closeness centrality, and degree of the disease

| No | Name | Betweenness centrality | Closeness centrality | Degree |
|---|---|---|---|---|
| 1 | Rheumatoid arthritis | 0.023199613 | 0.312960236 | 10 |
| 2 | Alzheimer disease | 0.031287725 | 0.350082372 | 23 |
| 3 | Diabetic complication | 0.083931122 | 0.36637931 | 28 |
| 4 | Prostate cancer | 0.001030997 | 0.281084656 | 3 |
| 5 | Chronic glaucoma | 0.005424507 | 0.306637807 | 10 |
| 6 | Stroke | 0.001111026 | 0.29109589 | 6 |
| 7 | Asthma | 0.047886814 | 0.362010221 | 32 |
| 8 | Breast cancer | 0.023479915 | 0.336767036 | 16 |
| 9 | Lupus | 7.23E+10 | 0.283711615 | 3 |
| 10 | Lipid metabolism disorder; Cardiovascular disease | 1.44E+12 | 0.276692708 | 3 |
| 11 | Attention deficit hyperactivity disorder | 0.010427305 | 0.307080925 | 21 |
| 12 | Depression | 0.001373707 | 0.289509537 | 15 |
| 13 | Hyperprolactinaemia | 0.003875351 | 0.288722826 | 13 |
| 14 | Glioma | 4.22E+12 | 0.282579787 | 12 |
| 15 | Schizophrenia | 0.023993075 | 0.323439878 | 25 |
| 16 | Spontaneous abortion | 0.001685171 | 0.289509537 | 20 |
| 17 | Hypertension | 0.002943421 | 0.29637378 | 9 |
| 18 | Cough | 0 | 0.254491018 | 1 |
| 19 | Congestive heart failure | 7.40E+11 | 0.28638814 | 13 |
| 20 | Cognitive impairment | 6.23E+10 | 0.274193548 | 7 |
| 21 | Chronic obstructive pulmonary disease | 0.001668414 | 0.272785623 | 2 |
| 22 | Follicular lymphoma | 0 | 0.263975155 | 1 |
| 23 | Cerebrovascular ischaemia | 0.002155619 | 0.283711615 | 4 |
| 24 | Breast cancer | 0.001698555 | 0.284471218 | 3 |
| 25 | Endotoxic shock | 0.00400527 | 0.292297111 | 4 |
| 26 | Genetic disease | 0 | 0.263975155 | 1 |
| 27 | Paroxysmal supraventricular tachycardia | 0 | 0.263975155 | 1 |
| 28 | Renal cell carcinoma | 0 | 0.263975155 | 1 |
| 29 | Hormone deficiency | 4.57E+11 | 0.279605263 | 3 |
| 30 | Lung cancer | 0 | 0.232240437 | 1 |
| 31 | Thrombosis | 0.001379314 | 0.288722826 | 5 |
| 32 | Bacterial infection | 0.002850776 | 0.299295775 | 8 |
| 33 | Inborn error of metabolism | 3.86E+12 | 0.279237845 | 4 |
| 34 | Myelofibrosis | 0 | 0.232240437 | 1 |
| 35 | Open-angle glaucoma | 0.001959702 | 0.29432133 | 6 |
| 36 | Fibrosis | 3.13E+12 | 0.279605263 | 4 |
| 37 | Ischemia | 0.002523969 | 0.295549374 | 7 |
| 38 | Melanoma | 0.002266947 | 0.287162162 | 5 |
| 39 | Parkinson disease | 4.51E+12 | 0.284471218 | 5 |
| 40 | Gout | 6.66E+11 | 0.283711615 | 4 |
| 41 | Cushing disease | 0.012433403 | 0.313884786 | 11 |
| 42 | Inflammatory bowel disease | 4.62E+09 | 0.246806039 | 2 |

| | | | | |
|---|---|---|---|---|
| 43 | Leishmaniasis | 4.62E+09 | 0.246806039 | 2 |
| 44 | Leukemia | 0.003816075 | 0.29109589 | 5 |
| 45 | Kidney Diseases | 1.59E+10 | 0.23957159 | 2 |
| 46 | Multiple myeloma | 1.59E+10 | 0.23957159 | 2 |
| 47 | Inflammation | 1.59E+10 | 0.23957159 | 2 |
| 48 | Essential thrombocythemia | 1.59E+10 | 0.23957159 | 2 |
| 49 | Polycythemia vera | 1.59E+10 | 0.23957159 | 2 |
| 50 | Anxiety disorder | 0.001420707 | 0.253579952 | 3 |
| 51 | Heart Failure | 0 | 0.257575758 | 1 |
| 52 | Myocardial Ischemia | 0.006505817 | 0.293914246 | 8 |
| 53 | Myocardial Infarction | 8.85E+09 | 0.267632242 | 4 |
| 54 | Hyperlipidemias | 8.85E+09 | 0.267632242 | 4 |
| 55 | Diabetic neuropathy | 3.16E+12 | 0.275974026 | 2 |
| 56 | Neuralgia | 5.79E+11 | 0.27997365 | 3 |
| 57 | Cardiovascular Diseases | 0.007646779 | 0.306195965 | 8 |
| 58 | Cardiovascular disease | 5.17E+10 | 0.279605263 | 3 |
| 59 | Haematological malignancy | 1.29E+11 | 0.262345679 | 2 |
| 60 | Hypotension | 0.003638136 | 0.300565771 | 6 |
| 61 | Ischemia | 0.001018328 | 0.277053455 | 3 |
| 62 | Angina pectoris | 0 | 0.24912075 | 1 |
| 63 | Atherosclerosis | 0 | 0.250589623 | 1 |
| 64 | Neoplasm Metastasis | 1.75E+12 | 0.261377614 | 2 |
| 65 | Intellectual Disability | 0 | 0.250589623 | 1 |
| 66 | Lateral sclerosis | 0 | 0.250589623 | 1 |
| 67 | Glycogen Storage Disease Type II | 8.36E+10 | 0.278871391 | 4 |
| 68 | Diabetes Mellitus, Type 2 | 1.49E+12 | 0.270700637 | 3 |
| 69 | Ataxia | 0 | 0.265625 | 1 |
| 70 | Acute myeloid leukaemia | 0.004646781 | 0.284852547 | 3 |
| 71 | Spinal muscular atrophy | 0 | 0.235587583 | 1 |
| 72 | Acute bronchial asthma | 0 | 0.235587583 | 1 |
| 73 | Dyslipidemia | 0 | 0.235587583 | 1 |
| 74 | Severe Acute Respiratory Syndrome | 0 | 0.235587583 | 1 |
| 75 | Acute myocardial infarction | 0 | 0.235587583 | 1 |
| 76 | Erythema | 0 | 0.235587583 | 1 |
| 77 | Pain | 0 | 0.239841986 | 1 |
| 78 | Acne vulgaris | 0.001036036 | 0.286002692 | 5 |
| 79 | Cholelithiasis | 0 | 0.239841986 | 1 |
| 80 | Diabetes Mellitus, Type 1 | 0 | 0.260736196 | 1 |
| 81 | Glucose Metabolism Disorders | 0 | 0.260736196 | 1 |
| 82 | Sucrase-isomaltase deficiency | 1.47E+12 | 0.268987342 | 3 |
| 83 | beta-Mannosidosis | 5.88E+10 | 0.267632242 | 2 |
| 84 | Autosomal Recessive | 1.47E+12 | 0.268987342 | 3 |
| 85 | Metabolic disorder | 1.19E+11 | 0.249413146 | 2 |
| 86 | Fabry disease | 0 | 0.247380675 | 1 |

| | | | | |
|---|---|---|---|---|
| 87 | Gangliosidosis, GM1 | 1.19E+11 | 0.249413146 | 2 |
| 88 | Cholangiocarcinoma | 6.46E+11 | 0.274193548 | 2 |
| 89 | Myotonic Dystrophy | 0 | 0.247380675 | 1 |
| 90 | Cell Transformation, Neoplastic | 0 | 0.247380675 | 1 |
| 91 | Discoid lupus erythematosus | 0 | 0.247380675 | 1 |
| 92 | Trigeminal Neuralgia | 0 | 0.247380675 | 1 |
| 93 | Thymic cancer | 4.70E+11 | 0.259146341 | 2 |
| 94 | Idiopathic pulmonary fibrosis | 0 | 0.247380675 | 1 |
| 95 | alpha-Mannosidosis | 0 | 0.248247664 | 1 |
| 96 | Crohn disease | 2.60E+12 | 0.275974026 | 2 |
| 97 | Hutchinson-Gilford progeria syndrome | 0 | 0.260736196 | 1 |
| 98 | Multiple Myeloma | 0 | 0.260736196 | 1 |
| 99 | Hepatic Fibrosis | 7.09E+10 | 0.272785623 | 2 |
| 100 | Neoplasm Invasiveness | 0 | 0.258201701 | 1 |
| 101 | Asthma | 0 | 0.258201701 | 1 |
| 102 | Anaplasia | 0 | 0.249706228 | 1 |
| 103 | Carbonic anhydrase va deficiency | 1.55E+10 | 0.271392082 | 2 |
| 104 | Breast Neoplasms | 0 | 0.252375297 | 1 |
| 105 | Hyperalgesia | 0 | 0.252375297 | 1 |
| 106 | Amino Acid Metabolism, Inborn Errors | 0 | 0.252375297 | 1 |
| 107 | Lung Neoplasms | 0 | 0.256024096 | 1 |
| 108 | Colonic Neoplasms | 0 | 0.256024096 | 1 |
| 109 | Leukemia | 7.75E+09 | 0.274547804 | 2 |
| 110 | Congenital chloride diarrhea | 0 | 0.259146341 | 1 |
| 111 | Obesity | 0 | 0.259146341 | 1 |
| 112 | Chemical and Drug Induced Liver Injury | 1.01E+12 | 0.266624843 | 2 |
| 113 | Non-Small-Cell Lung | 0 | 0.254491018 | 1 |
| 114 | Adenocarcinoma of Lung | 0 | 0.2319869 | 1 |
| 115 | Prostatic Neoplasms | 0 | 0.2319869 | 1 |

TABLE S5. Betweenness centrality, closeness centrality, and degree of the pathway

| No | Name | Betweenness centrality | Closeness centrality | Degree |
|---|---|---|---|---|
| 1 | Fructose and mannose metabolism | 0.003419483 | 0.299717913 | 8 |
| 2 | Oxidative phosphorylation | 0.031287725 | 0.350082372 | 23 |
| 3 | AGE-RAGE signaling pathway | 0.02616324 | 0.326923077 | 21 |
| 4 | Steroid hormone biosynthesis | 0.002882211 | 0.290697674 | 4 |
| 5 | Bacterial invasion of epithelial cells | 0.005424507 | 0.306637807 | 10 |
| 6 | Metabolism of proteins | 0.042596434 | 0.345528455 | 15 |
| 7 | Cytokine-cytokine receptor interaction | 0.06729194 | 0.377442274 | 34 |
| 8 | MAPK signaling pathway | 0.09828744 | 0.394248609 | 31 |
| 9 | Systemic lupus erythematosus | 7.23E+10 | 0.283711615 | 3 |

| | | | | |
|---|---|---|---|---|
| 10 | cAMP signaling pathway | 0.011551359 | 0.29637378 | 6 |
| 11 | Regulation of actin cytoskeleton | 0.00682588 | 0.298036466 | 18 |
| 12 | Calcium signaling pathway | 0.001373707 | 0.289509537 | 15 |
| 13 | Neuroactive ligand-receptor interaction | 0.040495946 | 0.332550861 | 23 |
| 14 | Adrenergic signaling in cardiomyocytes | 4.59E+10 | 0.271392082 | 5 |
| 15 | Inflammatory mediator regulation of TRP channels | 1.38E+12 | 0.268647282 | 2 |
| 16 | Adrenergic signaling in cardiomyocytes | 7.40E+11 | 0.28638814 | 13 |
| 17 | Regulation of actin cytoskeleton | 0.001428744 | 0.291895604 | 12 |
| 18 | Chemokine signaling pathway | 0.001668414 | 0.272785623 | 2 |
| 19 | Acute myeloid leukemia | 0.003714176 | 0.274547804 | 3 |
| 20 | Metabolism of lipids and lipoproteins | 0.002155619 | 0.283711615 | 16 |
| 21 | Estrogen signaling pathway | 0.006833995 | 0.303571429 | 7 |
| 22 | Metabolic pathways | 0.05786343 | 0.360169492 | 18 |
| 23 | Calcium signaling pathway | 0 | 0.263975155 | 1 |
| 24 | Citrate cycle (TCA cycle) | 0 | 0.263975155 | 1 |
| 25 | Signaling by Type 1 Insulin-like Growth Factor 1 Receptor (IGF1R) | 4.57E+11 | 0.279605263 | 3 |
| 26 | Hemostasis | 0 | 0.232240437 | 1 |
| 27 | Nitrogen metabolism | 0.002850776 | 0.299295775 | 8 |
| 28 | Metabolism | 3.86E+12 | 0.279237845 | 4 |
| 29 | Apoptosis | 5.65E+11 | 0.259146341 | 2 |
| 30 | Bacterial invasion of epithelial cells | 0.001959702 | 0.29432133 | 6 |
| 31 | Cellular responses to stress | 3.13E+12 | 0.279605263 | 4 |
| 32 | Tyrosine metabolism | 0.002266947 | 0.287162162 | 5 |
| 33 | Interleukin-1 signaling | 2.80E+11 | 0.278505898 | 3 |
| 34 | AGE-RAGE signaling pathway | 0 | 0.267969735 | 1 |
| 35 | Cytokine-cytokine receptor interaction | 4.62E+09 | 0.246806039 | 2 |
| 36 | AGE-RAGE signaling pathway | 4.96E+11 | 0.274902975 | 3 |
| 37 | Arachidonic acid metabolism | 4.62E+09 | 0.246806039 | 2 |
| 38 | Pathways in cancer | 0.005207229 | 0.29109589 | 5 |
| 39 | Signal Transduction | 0.046448729 | 0.351821192 | 19 |
| 40 | Complement and coagulation cascades | 4.19E+12 | 0.281084656 | 4 |
| 41 | Immune System | 0.005755067 | 0.281084656 | 4 |
| 42 | VEGF signaling pathway | 1.59E+10 | 0.23957159 | 2 |
| 43 | Signaling by Interleukins | 1.59E+10 | 0.23957159 | 2 |
| 44 | PI3K-Akt signaling pathway | 1.59E+10 | 0.23957159 | 2 |
| 45 | Jak-STAT signaling pathway | 0.00394087 | 0.278141361 | 3 |
| 46 | cGMP-PKG signaling pathway | 0 | 0.257575758 | 1 |
| 47 | Signal Transduction | 1.92E+10 | 0.268308081 | 5 |
| 48 | Cell adhesion molecules | 1.07E+12 | 0.277777778 | 6 |
| 49 | Thromboxane signalling through TP receptor | 8.85E+09 | 0.267632242 | 4 |
| 50 | Adrenoceptors | 8.85E+09 | 0.267632242 | 4 |
| 51 | Beta-Alanine metabolism | 0 | 0.257263923 | 1 |

| | | | | |
|---|---|---|---|---|
| 52 | Signaling by GPCR | 5.79E+11 | 0.27997365 | 3 |
| 53 | Metabolism | 0.004396942 | 0.298036466 | 5 |
| 54 | HDACs deacetylate histones | 0 | 0.24912075 | 1 |
| 55 | Alcoholism | 0 | 0.24912075 | 1 |
| 56 | Oxidative phosphorylation | 0 | 0.250589623 | 1 |
| 57 | Galactose metabolism | 8.36E+10 | 0.278871391 | 4 |
| 58 | Fluid shear stress and atherosclerosis | 0 | 0.250589623 | 1 |
| 59 | Alanine, aspartate and glutamate metabolism | 0 | 0.265625 | 1 |
| 60 | Inflammatory mediator regulation of TRP channels | 0 | 0.265625 | 1 |
| 61 | RNA transport | 0 | 0.235587583 | 1 |
| 62 | AMPK signaling pathway | 0 | 0.235587583 | 1 |
| 63 | Aldosterone-regulated sodium reabsorption | 0 | 0.235587583 | 1 |
| 64 | Vascular smooth muscle contraction | 0 | 0.235587583 | 1 |
| 65 | Arachidonic acid metabolism | 0 | 0.239841986 | 1 |
| 66 | Endocrine and other factor-regulated calcium reabsorption | 0.001036036 | 0.286002692 | 5 |
| 67 | Bile secretion | 0 | 0.239841986 | 1 |
| 68 | Lysosome | 5.88E+10 | 0.267632242 | 2 |
| 69 | Galactose metabolism | 1.19E+11 | 0.249413146 | 2 |
| 70 | Central carbon metabolism in cancer | 6.05E+11 | 0.258830694 | 2 |
| 71 | Cardiac conduction | 0 | 0.247380675 | 1 |
| 72 | Base excision repair | 6.04E+11 | 0.263647643 | 2 |
| 73 | Cell cycle | 4.70E+11 | 0.259146341 | 2 |
| 74 | Cell adhesion molecules | 0 | 0.258201701 | 1 |
| 75 | Nitrogen metabolism | 3.59E+11 | 0.278141361 | 4 |
| 76 | Signaling by Interleukins | 0 | 0.252375297 | 1 |
| 77 | Biosynthesis of amino acids | 0 | 0.252375297 | 1 |
| 78 | Bladder cancer | 2.96E+12 | 0.270356234 | 2 |
| 79 | Interleukin-1 signaling | 0 | 0.256024096 | 1 |
| 80 | Pancreatic secretion | 0 | 0.259146341 | 1 |
| 81 | nitrogen metabolism | 0 | 0.259146341 | 1 |
| 82 | Cysteine and methionine metabolism | 0 | 0.2319869 | 1 |

TABLE S6. Betweenness centrality, closeness centrality, and degree of protein-protein interaction

| No | Name | Betweenness centrality | Closeness centrality | Degree |
|---|---|---|---|---|
| 1 | GAPDH | 0.072068707 | 0.5776173 | 63 |
| 2 | VEGFA | 0.057751109 | 0.5714286 | 60 |
| 3 | MAPK3 | 0.067927382 | 0.5633803 | 59 |
| 4 | EGFR | 0.060625381 | 0.5633803 | 53 |
| 5 | STAT3 | 0.019287654 | 0.5387205 | 51 |
| 6 | HSP90AA1 | 0.041917216 | 0.5387205 | 49 |
| 7 | PTGS2 | 0.044649212 | 0.5405405 | 49 |
| 8 | ESR1 | 0.06313727 | 0.5387205 | 46 |

| | | | | |
|---|---|---|---|---|
| 9 | PPARG | 0.07471732 | 0.5333333 | 43 |
| 10 | MMP9 | 0.023815556 | 0.5144695 | 42 |
| 11 | IL2 | 0.028488024 | 0.5228758 | 38 |
| 12 | BCL2L1 | 0.007965098 | 0.5031447 | 37 |
| 13 | TLR4 | 0.016017596 | 0.5 | 36 |
| 14 | PIK3CA | 0.008553819 | 0.4984424 | 35 |
| 15 | JAK2 | 0.01138248 | 0.4938272 | 33 |
| 16 | SLC6A4 | 0.074537741 | 0.4833837 | 32 |
| 17 | MAPK8 | 0.004139932 | 0.4984424 | 32 |
| 18 | NR3C1 | 0.054204486 | 0.516129 | 32 |
| 19 | MMP2 | 0.003707481 | 0.4819277 | 31 |
| 20 | MCL1 | 0.003439778 | 0.4651163 | 29 |
| 21 | PGR | 0.009111226 | 0.4819277 | 29 |
| 22 | KIT | 0.004778716 | 0.4790419 | 28 |
| 23 | SLC6A3 | 0.050810121 | 0.4705882 | 28 |
| 24 | TGFB1 | 0.004806835 | 0.4776119 | 27 |
| 25 | IGF1R | 0.001799129 | 0.4819277 | 27 |
| 26 | PRKCD | 0.010414657 | 0.4705882 | 26 |
| 27 | AR | 0.009138756 | 0.4719764 | 25 |
| 28 | JAK1 | 0.005598122 | 0.4610951 | 25 |
| 29 | SLC6A2 | 0.019120665 | 0.4113111 | 24 |
| 30 | CDK2 | 0.004442882 | 0.4664723 | 23 |
| 31 | GSK3B | 0.003048005 | 0.4747774 | 23 |
| 32 | HDAC1 | 0.008411824 | 0.4819277 | 23 |
| 33 | SERPINE1 | 0.002604211 | 0.4678363 | 23 |
| 34 | MPO | 0.004210974 | 0.4519774 | 23 |
| 35 | MAOA | 0.015859067 | 0.4301075 | 22 |
| 36 | PRKCA | 0.0121799 | 0.4907975 | 22 |
| 37 | PTPN1 | 0.012343099 | 0.4705882 | 22 |
| 38 | JAK3 | 0.003405998 | 0.4395604 | 21 |
| 39 | NOS2 | 0.016745381 | 0.4651163 | 20 |
| 40 | ADRB2 | 0.035182575 | 0.495356 | 20 |
| 41 | PPP2CA | 0.015929494 | 0.4705882 | 20 |
| 42 | PRKCE | 0.018570687 | 0.4637681 | 20 |
| 43 | CYP19A1 | 0.009653477 | 0.4584527 | 19 |
| 44 | IDH1 | 0.010952491 | 0.4221636 | 18 |
| 45 | MMP1 | 0.011389356 | 0.4519774 | 18 |
| 46 | CDK6 | 7.34E-04 | 0.4407713 | 18 |
| 47 | PIK3CB | 8.35E-04 | 0.4244032 | 17 |
| 48 | CA9 | 0.024858643 | 0.4432133 | 17 |
| 49 | AKR1B1 | 0.036097706 | 0.4637681 | 17 |
| 50 | ESR2 | 0.003951425 | 0.4545455 | 17 |
| 51 | MAPK9 | 8.94E-04 | 0.4444444 | 17 |
| 52 | F2 | 0.010114125 | 0.4494382 | 17 |
| 53 | FLT3 | 0.001153348 | 0.4289544 | 16 |

| | | | | |
|---|---|---|---|---|
| 54 | FLT1 | 6.03E-04 | 0.4371585 | 16 |
| 55 | DRD2 | 0.010907104 | 0.4584527 | 15 |
| 56 | ABCG2 | 0.011116949 | 0.4347826 | 15 |
| 57 | ALK | 3.75E-04 | 0.4383562 | 15 |
| 58 | MGAM | 0.016665931 | 0.4166667 | 15 |
| 59 | MAPK10 | 0.001846747 | 0.4188482 | 14 |
| 60 | SI | 0.0143962 | 0.4134367 | 14 |
| 61 | ELANE | 0.002705949 | 0.4092072 | 14 |
| 62 | OPRM1 | 0.015860046 | 0.4407713 | 14 |
| 63 | ADORA2A | 0.015606885 | 0.4532578 | 13 |
| 64 | TBXA2R | 0.009597399 | 0.4188482 | 13 |
| 65 | ALDH2 | 0.014480515 | 0.4507042 | 13 |
| 66 | ARG1 | 3.58E-04 | 0.4278075 | 13 |
| 67 | ALOX5 | 0.002813818 | 0.4123711 | 13 |
| 68 | BCL2 | 2.92E-04 | 0.4145078 | 13 |
| 69 | GBA | 0.036162597 | 0.4395604 | 13 |
| 70 | F3 | 0.001650384 | 0.4210526 | 13 |
| 71 | CDC25A | 9.91E-04 | 0.4232804 | 13 |
| 72 | NOX4 | 7.39E-04 | 0.4278075 | 13 |
| 73 | ADORA1 | 0.010136302 | 0.4432133 | 13 |
| 74 | GLB1 | 0.005438733 | 0.361991 | 13 |
| 75 | HTR1A | 0.010836946 | 0.4071247 | 12 |
| 76 | ACHE | 0.020517538 | 0.4395604 | 12 |
| 77 | PRKCG | 0.003644139 | 0.4301075 | 12 |
| 78 | DRD1 | 0.004604181 | 0.3773585 | 11 |
| 79 | GLA | 0.003503944 | 0.3603604 | 11 |
| 80 | ADRA1B | 0.006143319 | 0.4166667 | 11 |
| 81 | ADK | 0.002804078 | 0.3678161 | 10 |
| 82 | HTR2A | 0.001592668 | 0.3931204 | 10 |
| 83 | LDHA | 0.003444853 | 0.4336043 | 10 |
| 84 | ADRA2A | 0.002784239 | 0.3960396 | 10 |
| 85 | ADORA2B | 0.004325788 | 0.4166667 | 10 |
| 86 | PLA2G1B | 0.001348901 | 0.4102564 | 9 |
| 87 | MMP12 | 1.17E-04 | 0.4102564 | 9 |
| 88 | CYP1B1 | 4.87E-04 | 0.4347826 | 9 |
| 89 | ADRA2C | 0.002022301 | 0.3940887 | 9 |
| 90 | MANBA | 8.76E-04 | 0.3361345 | 9 |
| 91 | ROCK2 | 2.17E-04 | 0.4113111 | 9 |
| 92 | PLA2G2A | 0.004410631 | 0.4081633 | 9 |
| 93 | ADA | 0.004992618 | 0.3902439 | 9 |
| 94 | HTR5A | 8.47E-04 | 0.3426124 | 9 |
| 95 | HTR2C | 0.002036741 | 0.3864734 | 9 |
| 96 | DRD4 | 9.80E-04 | 0.3755869 | 9 |
| 97 | SLC29A1 | 0.001414587 | 0.3478261 | 8 |

| | | | | |
|---|---|---|---|---|
| 98 | MAN2B1 | 8.66E-04 | 0.3354298 | 8 |
| 99 | PIM2 | 2.19E-04 | 0.3809524 | 8 |
| 100 | TYR | 0.003554552 | 0.4312668 | 8 |
| 101 | SIGMAR1 | 0.004047615 | 0.3755869 | 8 |
| 102 | ADORA3 | 0.00381054 | 0.4324324 | 8 |
| 103 | CCR1 | 5.26E-05 | 0.3921569 | 8 |
| 104 | TBXAS1 | 0.002104146 | 0.4040404 | 8 |
| 105 | UGCG | 0.007703922 | 0.3940887 | 8 |
| 106 | PDE4A | 9.45E-04 | 0.383693 | 7 |
| 107 | GANAB | 0.00403321 | 0.334728 | 7 |
| 108 | LDHB | 0.002555428 | 0.4188482 | 7 |
| 109 | AOC3 | 0.002362426 | 0.4221636 | 7 |
| 110 | HTR1B | 2.02E-04 | 0.3485839 | 7 |
| 111 | HTR1D | 0.001662078 | 0.3603604 | 7 |
| 112 | ALOX15 | 3.87E-04 | 0.3800475 | 7 |
| 113 | PRKCH | 0.002652949 | 0.3931204 | 7 |
| 114 | XDH | 0.003821737 | 0.3883495 | 7 |
| 115 | DRD5 | 0.001033359 | 0.3547672 | 7 |
| 116 | PIM1 | 1.89E-04 | 0.3990025 | 6 |
| 117 | DRD3 | 5.67E-05 | 0.3470716 | 6 |
| 118 | ALOX12 | 3.81E-04 | 0.369515 | 6 |
| 119 | ADRA1D | 4.78E-04 | 0.3652968 | 6 |
| 120 | TRPA1 | 0.0010905 | 0.3508772 | 6 |
| 121 | HRH3 | 0.001580526 | 0.3555556 | 6 |
| 122 | ADRA1A | 4.78E-04 | 0.3652968 | 6 |
| 123 | OPRD1 | 7.21E-04 | 0.3874092 | 6 |
| 124 | GAA | 9.83E-06 | 0.3007519 | 6 |
| 125 | HSD11B1 | 9.32E-04 | 0.383693 | 6 |
| 126 | FUCA1 | 8.09E-04 | 0.3333333 | 6 |
| 127 | HTR2B | 3.49E-05 | 0.3470716 | 6 |
| 128 | SERPINA6 | 9.28E-04 | 0.372093 | 6 |
| 129 | OPRK1 | 0.001790384 | 0.4266667 | 6 |
| 130 | CYP11B1 | 0.001155086 | 0.3703704 | 5 |
| 131 | DAPK1 | 6.05E-06 | 0.4010025 | 5 |
| 132 | ADRB1 | 0.001520123 | 0.4081633 | 5 |
| 133 | HSD11B2 | 9.75E-05 | 0.3547672 | 5 |
| 134 | PPM1B | 2.63E-04 | 0.3800475 | 5 |
| 135 | KLKB1 | 0.00123536 | 0.3669725 | 5 |
| 136 | SLC5A2 | 0.005113776 | 0.39801 | 5 |
| 137 | HTR7 | 6.46E-04 | 0.3426124 | 5 |
| 138 | CA4 | 0.00175775 | 0.3397028 | 4 |
| 139 | CSNK2A1 | 3.67E-05 | 0.3809524 | 4 |
| 140 | HMGCR | 8.10E-04 | 0.3970223 | 4 |
| 141 | GBA2 | 2.37E-04 | 0.3305785 | 4 |

| | | | | |
|---|---|---|---|---|
| 142 | CA2 | 0.008124251 | 0.3539823 | 4 |
| 143 | AKR1B10 | 7.10E-04 | 0.3501094 | 4 |
| 144 | TRPM8 | 2.44E-04 | 0.3455724 | 4 |
| 145 | EPHX2 | 5.16E-04 | 0.3375527 | 4 |
| 146 | CA1 | 0.006835904 | 0.3470716 | 4 |
| 147 | ALPL | 0.004640392 | 0.391198 | 4 |
| 148 | ABCC1 | 7.75E-04 | 0.3902439 | 4 |
| 149 | CA12 | 0.001324298 | 0.3628118 | 4 |
| 150 | AVPR2 | 0 | 0.3921569 | 3 |
| 151 | METAP2 | 0 | 0.3940887 | 3 |
| 152 | DDO | 0 | 0.3319502 | 3 |
| 153 | SLC5A1 | 3.58E-04 | 0.3782506 | 3 |
| 154 | CA14 | 0 | 0.3131115 | 3 |
| 155 | ADRB3 | 1.98E-04 | 0.3747073 | 3 |
| 156 | SLC22A12 | 3.86E-04 | 0.3389831 | 3 |
| 157 | CA7 | 0 | 0.2821869 | 2 |
| 158 | HTR6 | 0 | 0.3292181 | 2 |
| 159 | HTR1F | 0 | 0.3265306 | 1 |
| 160 | HCAR2 | 0 | 0.3485839 | 1 |
| 161 | MPG | 0 | 0.3508772 | 1 |
| 162 | CA6 | 0 | 0 | 0 |
| 163 | PTPRCAP | 0 | 0 | 0 |
| 164 | ABCC9 | 0 | 0 | 0 |

TABLE S7. Receptor targets, binding affinity, and amino acid residues on molecular docking analysis. Bold letters indicate hydrogen bonds formed between the ligand–receptors

| No | Ligand | Target | Binding affinity (kcal $mol^{-1}$) | Amino acid residues |
|---|---|---|---|---|
| 1 | p-Coumaric acid | HCAR2 | -6,2 | Ser61, Phe65, Val120, Val120, **Asp124**, Phe127, Arg128, Asn137, Leu136, Ile139, Ile147 |
| 2 | Methyl nicotinate | HCAR2 | -5,4 | Ser61, Phe65, Val120, Asn124, Phe127, Arg128, **Leu136**, Ile139, Asn137, Ile147 |
| 3 | Cinnamic acid | HCAR2 | -6,1 | **Ser61**, Phe65, Val120, Val123, **Asp124**, Phe127, Arg128, Leu136, Asn137, Ile139, Ile147 |
| 4 | Muricatacin | HMGCR | -5,9 | Ala564, Tyr479, **Arg495**, Lys480, Gly542, Asn567, Arg568, Glu528, **Val530**, Met523, Gly524, **Asn529** |
| 5 | Coronin | PTGS2 | -7,5 | His39, Cys41, Arg44, Gly45, Val46, **Cys47**, **Tyr130**, Gly135, Lys137, Leu152, Pro153, Gln461, Glu465, Arg469 |
| 6 | (-)-Loliolide | PTGS2 | -7,0 | Tyr348, Val349, Leu352, Val523, Ala527 |
| 7 | (+)-Isololiolide | PTGS2 | -5,8 | His207, Phe210, **Thr212**, His214, Asn382, Tyr385, His386, His388, Val447, Gln454 |
| 8 | Coclaurine | ADRB3 | -8,9 | **Tyr59**, Ala60, Met101, Thr102, Ser147, **Arg150**, Asn230, Gln236, Thr274, Ser275, Arg314, Ser316, Cys317, **Leu318**, Trp332 |

| | | | | |
|---|---|---|---|---|
| 9 | Anomuricine | ADRB3 | -8,0 | **Tyr59**, Ala60, Met61, **Met101**, Thr102, Ser147, Met188, Ser189, Asn230, Ala231, Lys233, Gln236, Thr274, Ser275, Val276, Arg314, Ser316, Cys317, Leu318 |
| 10 | (+)-Anomurine | ADRB3 | -6,9 | Ala60, Met61, His62, Trp63, Arg150, **Ser191**, Leu192, Pro194, Leu19, Phe234, Cys233, Val276, Pro236, Val276, Ser277, Phe278, Cys317, Leu318, Gly319, **Val320** |
| 11 | Anomurine | ADRB3 | -7,6 | Ala48, Asp49, Asn50, Ser51, Asp5, Asn35, Gly52, Cys107, Trp47, Asp109, Phe108, Thr111, Val110, Arg231, Asp229, Glu258, **Arg255**, Asn261, Ala259, Ser265, Leu262, |
| 12 | Coclaurine | ADRB2 | -7,9 | Leu1013, Lys1060, Ile1050, Glu1064, Ala1063, Ile1029, Asp1061, Glu1062, Lys1065, Leu1066, Phe1067, Asn1068 |
| 13 | Anomuricine | ADRB2 | -7,1 | Glu1011, Tyr1018, **Asp1020**, **Glu1022**, Tyr1024, Leu1032, Gly1030, Asp1070, Thr1026, His1031, Phe1104, Gln1105 |
| 14 | (+)-Anomurine | ADRB2 | -7,1 | Glu1011, **Asp1020**, Glu1022, Leu1032, **Gln1105**, **Arg1145** |
| 15 | Anomurine | ADRB2 | -7,0 | Glu1011, Tyr1018, **Asp1020**, Thr1026, **Gly1030**, Leu1032, Glu1022, Tyr1024, His1031, Asp1070, Phe1104, Gln1105 |
| 16 | N-methylcoclaurine | ADRB2 | -7,9 | Glu1011, Asp1020, Glu1022, Thr1026, **Gly1030**, His1031, Leu1032, Asp1070, Val1071, Ala1074, Phe1104, Gln1105, Gly1107 |
| 17 | (Z)-3-Hexenyl beta-D-glucopyranoside | VEGFA | -6,0 | Phe36, **Leu66** |
| 18 | Kaempferol | XDH | -8,3 | Leu228, Thr229, **Cys285**, Arg288, **Ile326**, Met329, Leu330, Leu333 |
| 19 | Quercetin | XDH | -9,3 | Phe226, Cys285, Gln286, Leu228, Arg288, **Ser289**, Ala292, Glu295, Ile326, Tyr327, Met329, Leu330, Leu340, Leu333, Ile341, Phe363, Met364 |
| 20 | Emodin | XDH | -7,1 | Tyr222, Phe226, Pro227, Leu228, Thr229, Cys285, Arg288, Glu295, Leu330, Leu333, Ile326, **Met329**, Ser332, Ile341, Ser342 |
| 21 | Fisetin | XDH | -8,8 | Tyr222, Phe226, Pro227, Leu228, Thr229, Cys285, Arg288, Glu295, **Ile326**, **Met329**, Leu330, Ser332, Leu333, Ile341, Ser342 |
| 22 | Glycitein | XDH | -8,4 | Tyr222, Phe226, **Leu228**, Thr229, Lys230, Tyr222, Cys285, Ser289, Arg288, Ala292, Glu295, Met329, Leu330, Ser332, Leu333 |
| 23 | Morin | XDH | -8,6 | Tyr222, Phe226, **Leu228**, Thr229, Cys285, Arg288, Ser289, Ala292, Glu295, Ile326, Met329, Leu330, Ser332, Leu333, Leu340 |
| 24 | Robinetin | XDH | -8,8 | Tyr222, Phe226, Pro227, **Leu228**, Thr229, Cys285, Arg288, **Glu295**, **Ile326**, Met329, Leu330, Ser332, Leu333, Ile341, Ser342, Glu343 |

a

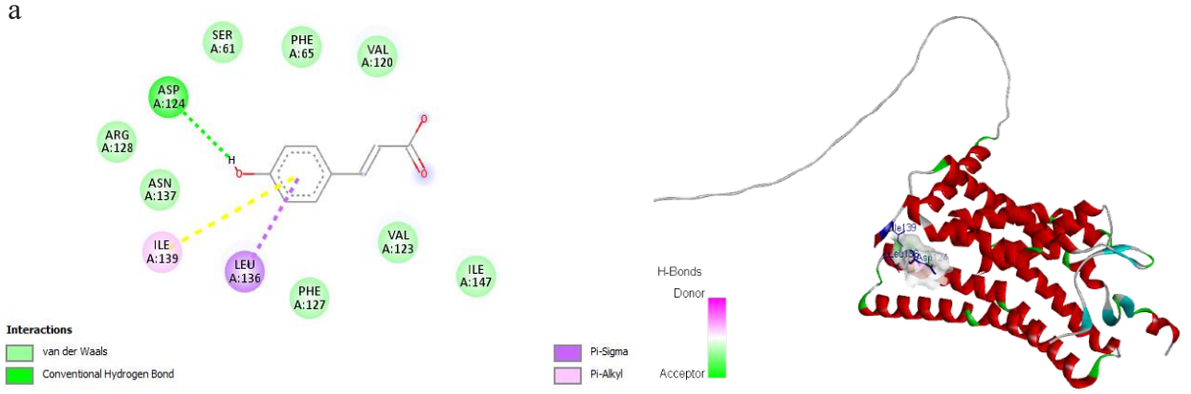
SER A:61
PHE A:65
VAL A:120
ASP A:124
ARG A:128
ASN A:137
ILE A:139
LEU A:136
PHE A:127
VAL A:123
ILE A:147
Interactions
van der Waals
Conventional Hydrogen Bond
Pi-Sigma
Pi-Alkyl
H-Bonds
Donor
Acceptor

b


VAL A:120
ILE A:139
ASN A:137
ILE A:147
PHE A:65
VAL A:123
LEU A:136
SER A:61
ASP A:124
ARG A:128
PHE A:127
Interactions
van der Waals
Salt Bridge
Conventional Hydrogen Bond
Carbon Hydrogen Bond
H-Bonds
Donor
Acceptor

c

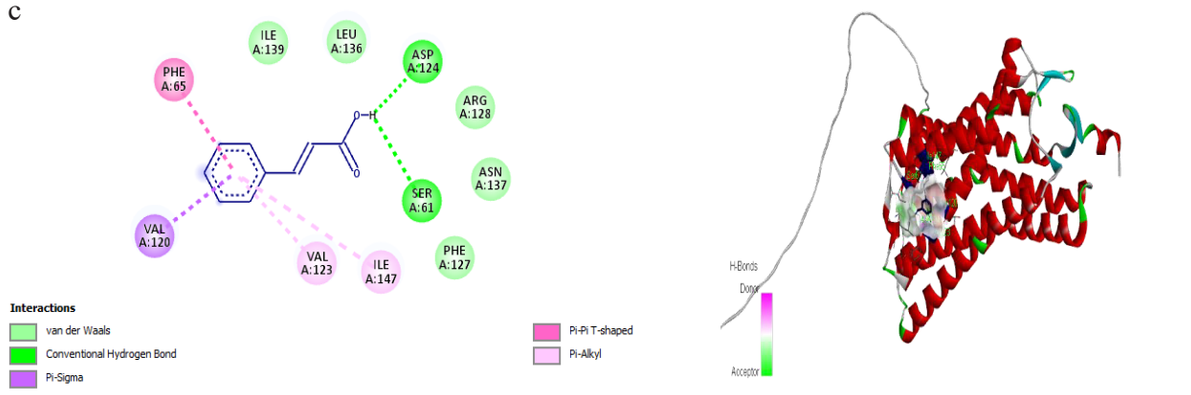
ILE A:139
LEU A:136
PHE A:65
ASP A:124
ARG A:128
ASN A:137
SER A:61
VAL A:120
VAL A:123
ILE A:147
PHE A:127
Interactions
van der Waals
Conventional Hydrogen Bond
Pi-Sigma
Pi-Pi T-shaped
Pi-Alkyl
H-Bonds
Donor
Acceptor

d

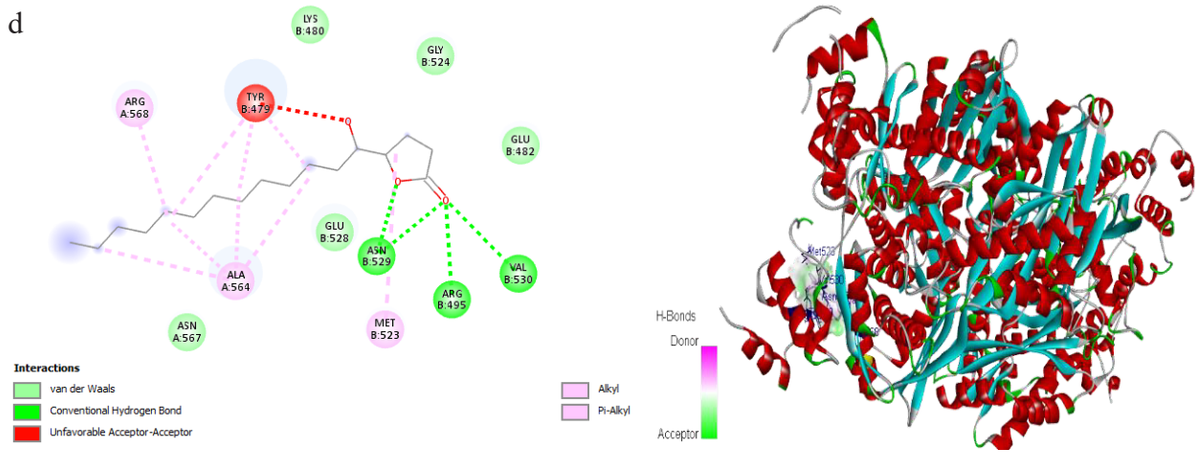
LYS B:480
GLY B:524
ARG A:568
TYR B:479
GLU B:482
GLU B:528
ASN B:529
VAL B:530
ALA A:564
ARG B:495
ASN A:567
MET B:523
Interactions
van der Waals
Conventional Hydrogen Bond
Unfavorable Acceptor-Acceptor
Alkyl
Pi-Alkyl
H-Bonds
Donor
Acceptor

e

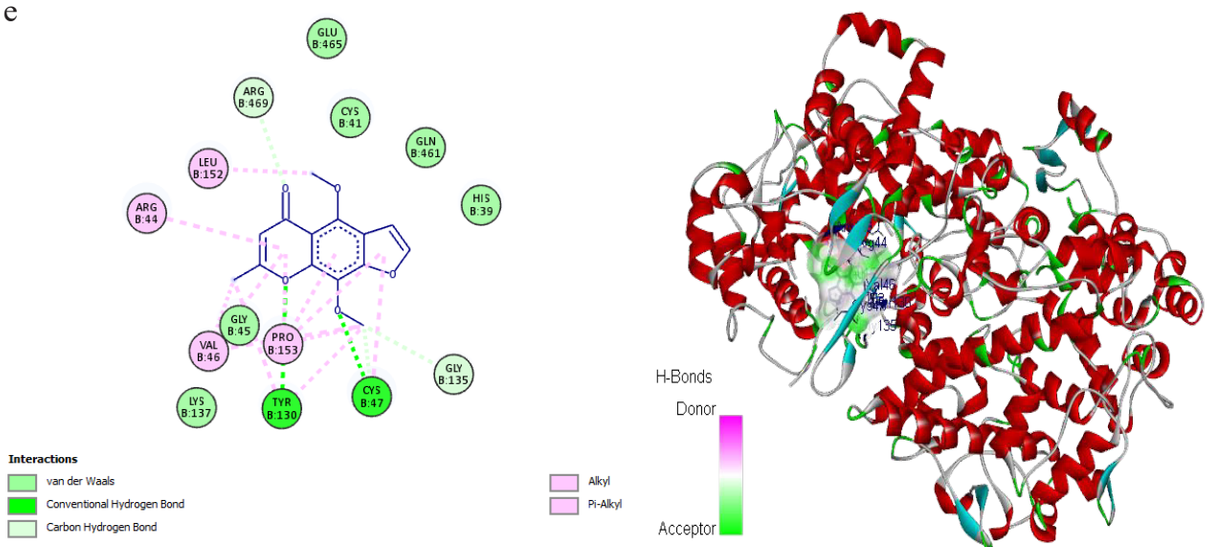
GLU B:465
ARG B:469
CYS B:41
GLN B:461
LEU B:152
HIS B:39
ARG B:44
GLY B:45
VAL B:46
PRO B:153
GLY B:135
LYS B:137
TYR B:130
CYS B:47
Interactions
van der Waals
Conventional Hydrogen Bond
Carbon Hydrogen Bond
Alkyl
Pi-Alkyl
H-Bonds
Donor
Acceptor

f

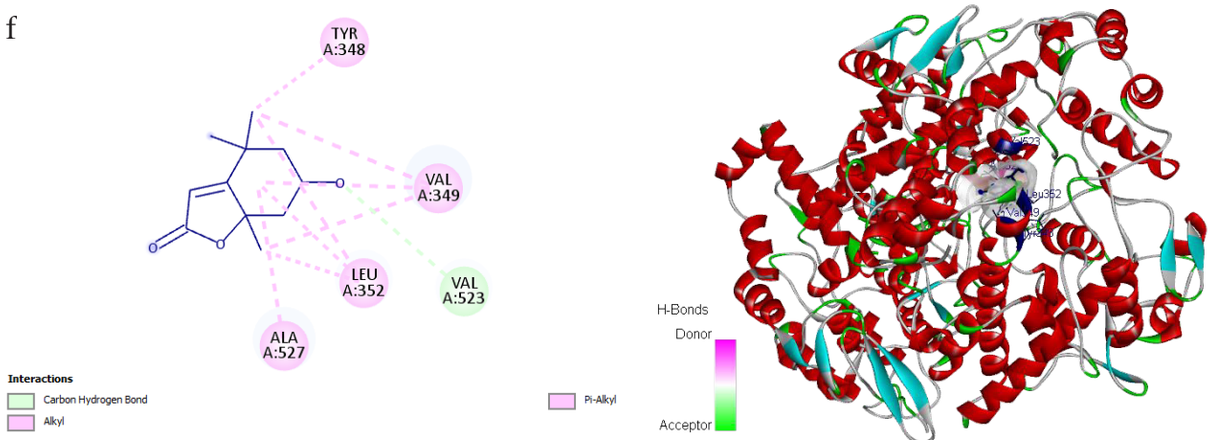
TYR A:348
VAL A:349
LEU A:352
VAL A:523
ALA A:527
Interactions
Carbon Hydrogen Bond
Alkyl
Pi-Alkyl
H-Bonds
Donor
Acceptor

g

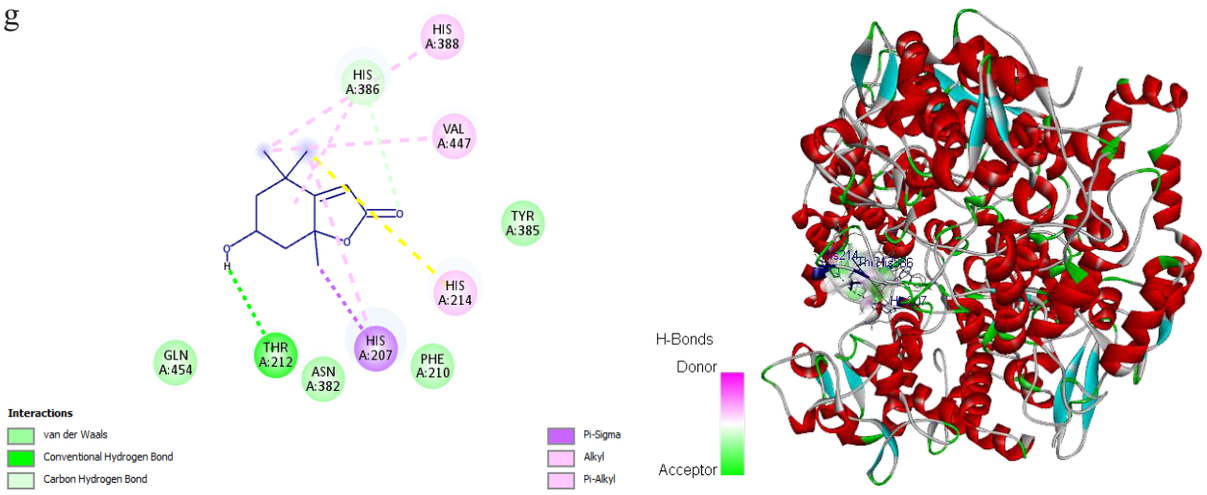
HIS A:388
HIS A:386
VAL A:447
TYR A:385
HIS A:214
GLN A:454
THR A:212
HIS A:207
PHE A:210
ASN A:382
Interactions
van der Waals
Conventional Hydrogen Bond
Carbon Hydrogen Bond
Pi-Sigma
Alkyl
Pi-Alkyl
H-Bonds
Donor
Acceptor

h

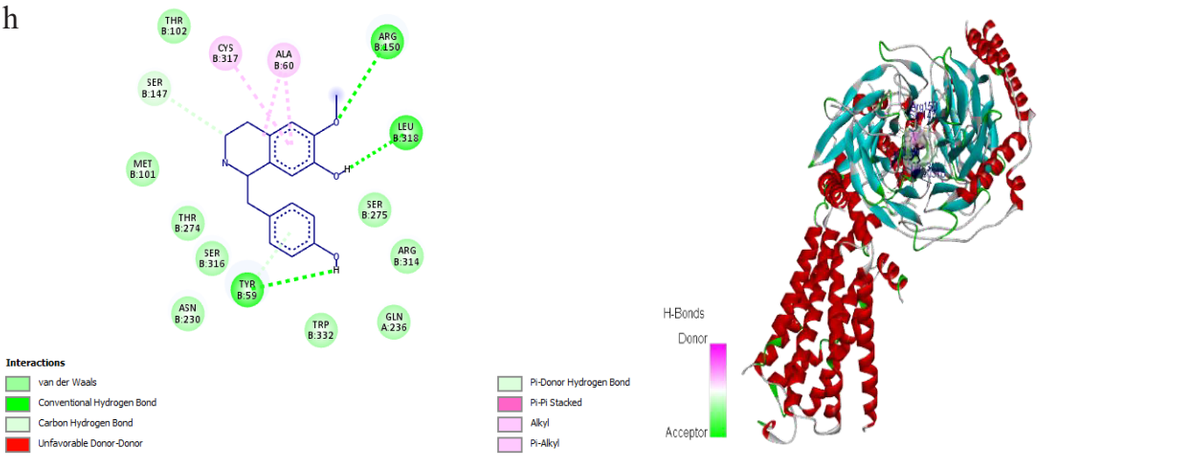
THR B:102
CYS B:317
ALA B:60
ARG B:450
SER B:147
LEU B:318
MET B:101
SER B:275
THR B:274
SER B:316
ARG B:314
TYR B:59
ASN B:230
TRP B:332
GLN A:236
Interactions
van der Waals
Conventional Hydrogen Bond
Carbon Hydrogen Bond
Unfavorable Donor-Donor
Pi-Donor Hydrogen Bond
Pi-Pi Stacked
Alkyl
Pi-Alkyl
H-Bonds
Donor
Acceptor

i

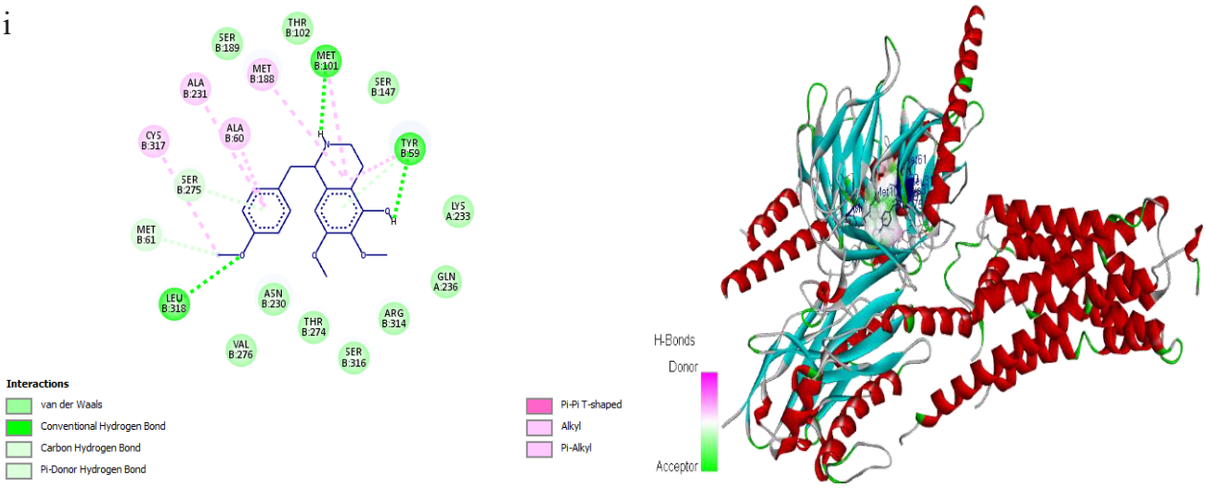
THR B:102
SER B:189
MET B:101
MET B:188
ALA B:231
SER B:147
ALA B:60
CYS B:317
TYR B:59
SER B:275
LYS A:233
MET B:61
GLN A:236
LEU B:318
ASN B:230
ARG B:314
THR B:274
VAL B:276
SER B:316
Interactions
van der Waals
Conventional Hydrogen Bond
Carbon Hydrogen Bond
Pi-Donor Hydrogen Bond
Pi-Pi T-shaped
Alkyl
Pi-Alkyl
H-Bonds
Donor
Acceptor

j

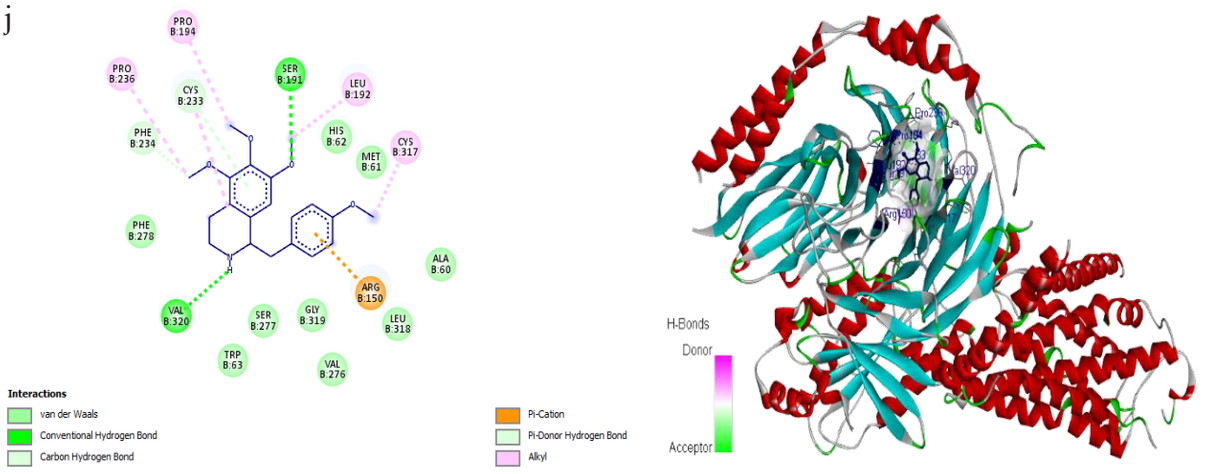
PRO B:194
PRO B:236
SER B:191
LEU B:192
CYS B:233
PHE B:234
HIS B:62
CYS B:317
MET B:61
PHE B:278
ALA B:60
ARG B:150
VAL B:320
SER B:277
GLY B:319
LEU B:318
TRP B:63
VAL B:276
Interactions
van der Waals
Conventional Hydrogen Bond
Carbon Hydrogen Bond
Pi-Cation
Pi-Donor Hydrogen Bond
Alkyl
H-Bonds
Donor
Acceptor

k

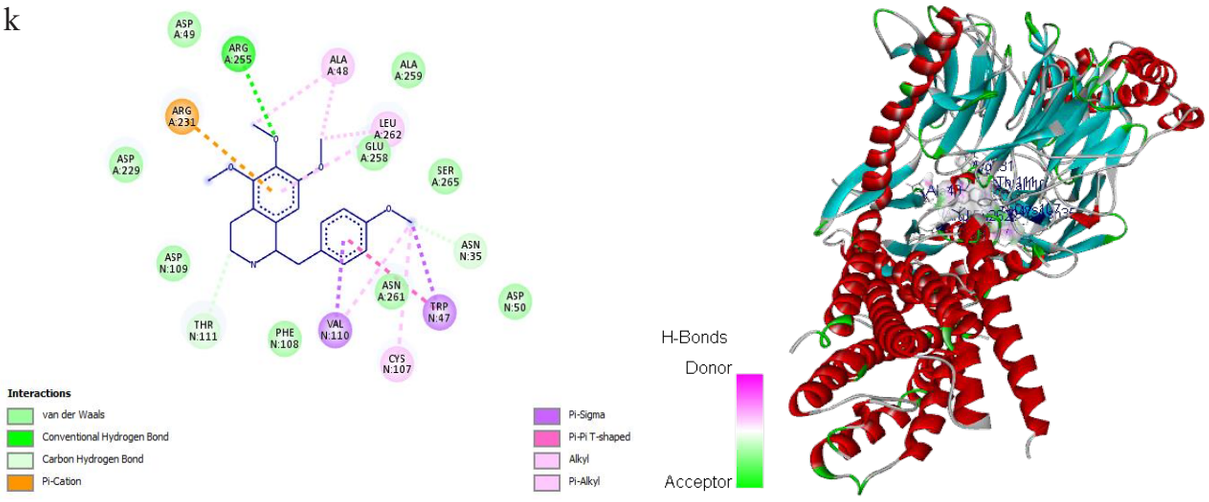
ASP A:49
ARG A:255
ALA A:48
ALA A:259
ARG A:231
LEU A:262
GLU A:258
ASP A:229
SER A:265
ASN N:35
ASP N:109
ASN A:261
TRP N:47
ASP N:50
THR N:111
PHE N:108
VAL N:110
CYS N:107
Interactions
van der Waals
Conventional Hydrogen Bond
Carbon Hydrogen Bond
Pi-Cation
Pi-Sigma
Pi-Pi T-shaped
Alkyl
Pi-Alkyl
H-Bonds
Donor
Acceptor

l

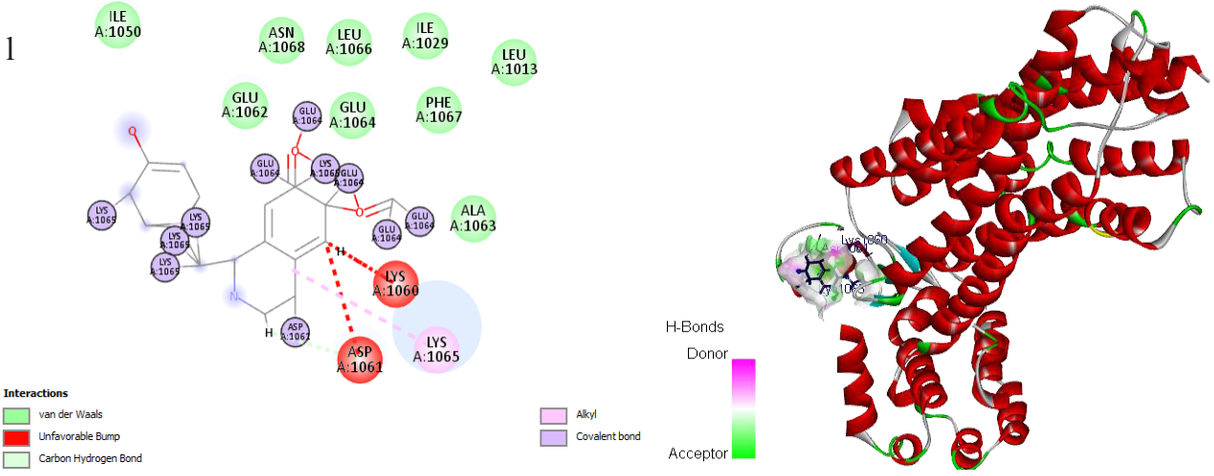
ILE A:1050
ASN A:1068
LEU A:1066
ILE A:1029
LEU A:1013
GLU A:1062
GLU A:1064
PHE A:1067
ALA A:1063
LYS A:1060
LYS A:1065
ASP A:1061
Interactions
van der Waals
Unfavorable Bump
Carbon Hydrogen Bond
Alkyl
Covalent bond
H-Bonds
Donor
Acceptor

m

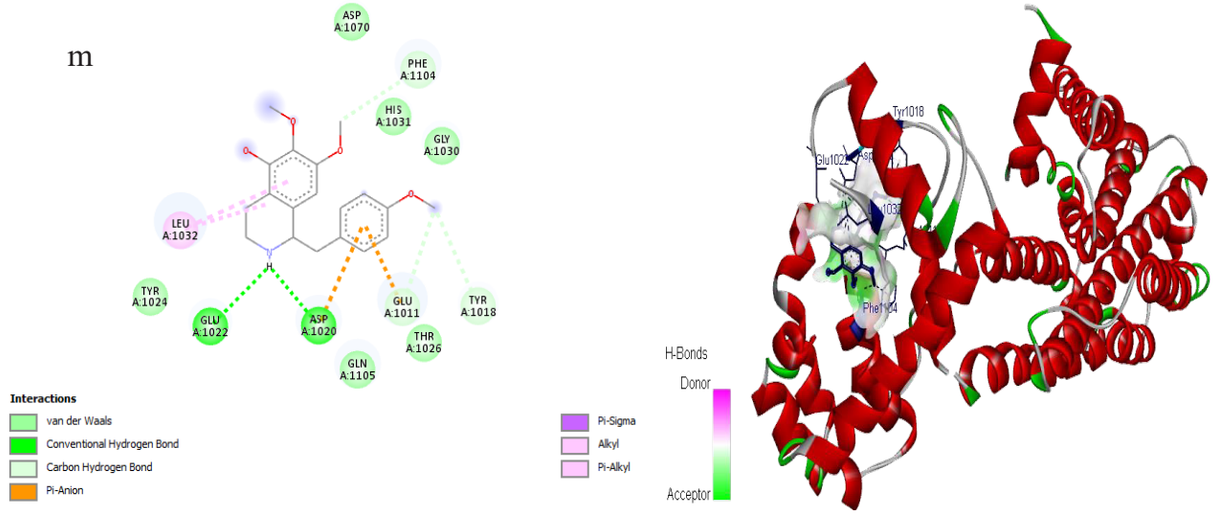
ASP A:1070
PHE A:1104
HIS A:1031
GLY A:1030
LEU A:1032
TYR A:1024
GLU A:1022
ASP A:1020
GLU A:1011
TYR A:1018
THR A:1026
GLN A:1105
Tyr1018
Interactions
van der Waals
Conventional Hydrogen Bond
Carbon Hydrogen Bond
Pi-Anion
Pi-Sigma
Alkyl
Pi-Alkyl
H-Bonds
Donor
Acceptor

n

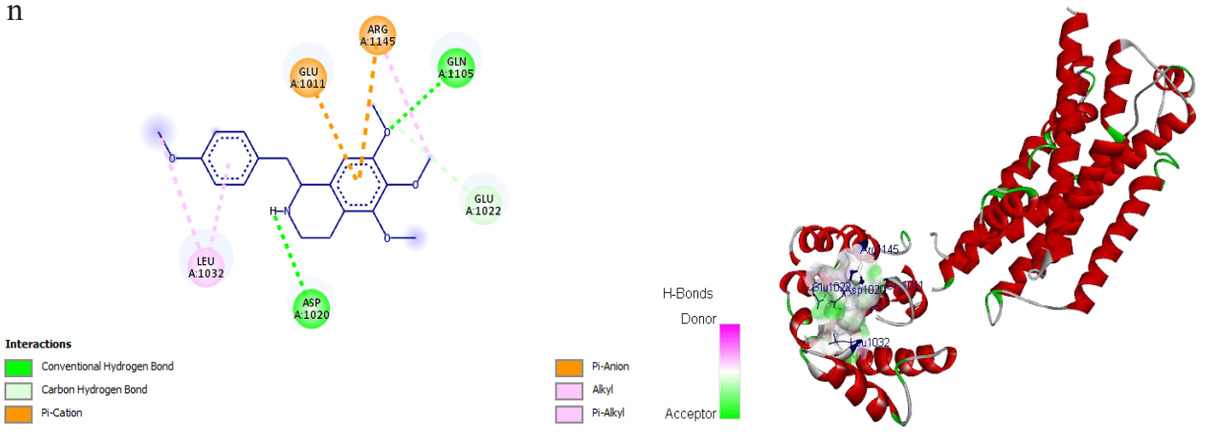
ARG A:1145
GLU A:1011
GLN A:1105
GLU A:1022
LEU A:1032
ASP A:1020
Interactions
Conventional Hydrogen Bond
Carbon Hydrogen Bond
Pi-Cation
Pi-Anion
Alkyl
Pi-Alkyl
H-Bonds
Donor
Acceptor

o

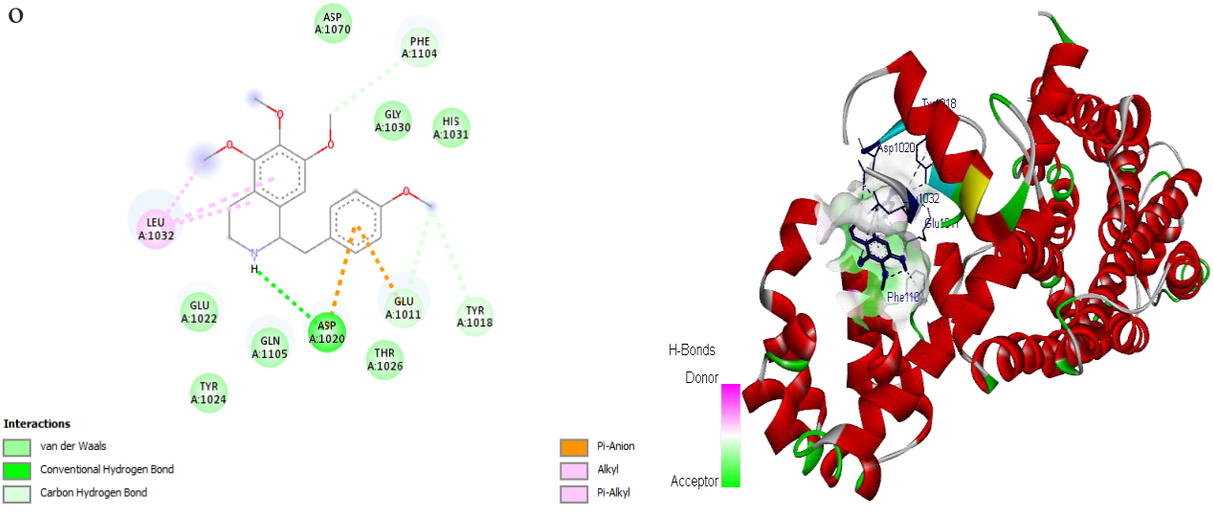
ASP A:1070
PHE A:1104
GLY A:1030
HIS A:1031
LEU A:1032
GLU A:1022
GLN A:1105
ASP A:1020
GLU A:1011
TYR A:1018
THR A:1026
TYR A:1024
Interactions
van der Waals
Conventional Hydrogen Bond
Carbon Hydrogen Bond
Pi-Anion
Alkyl
Pi-Alkyl
H-Bonds
Donor
Acceptor

p

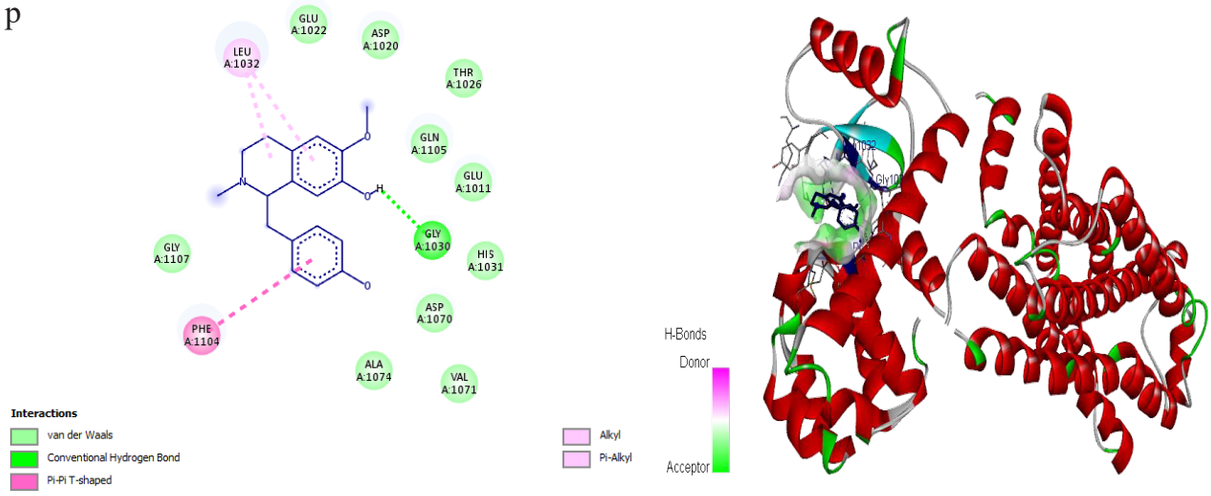
GLU A:1022
ASP A:1020
LEU A:1032
THR A:1026
GLN A:1105
GLU A:1011
GLY A:1030
GLY A:1107
HIS A:1031
ASP A:1070
PHE A:1104
ALA A:1074
VAL A:1071
Interactions
van der Waals
Conventional Hydrogen Bond
Pi-Pi T-shaped
Alkyl
Pi-Alkyl
H-Bonds
Donor
Acceptor

q

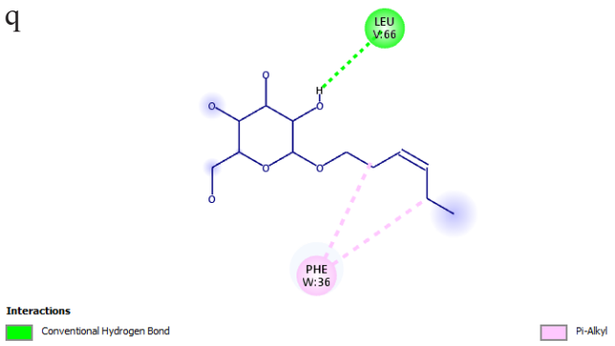
LEU
V:66
PHE
W:36
Interactions
Conventional Hydrogen Bond
Pi-Alkyl

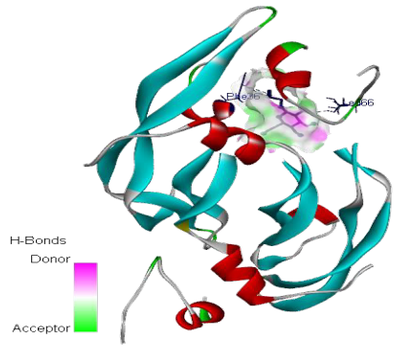
H-Bonds
Donor
Acceptor

r

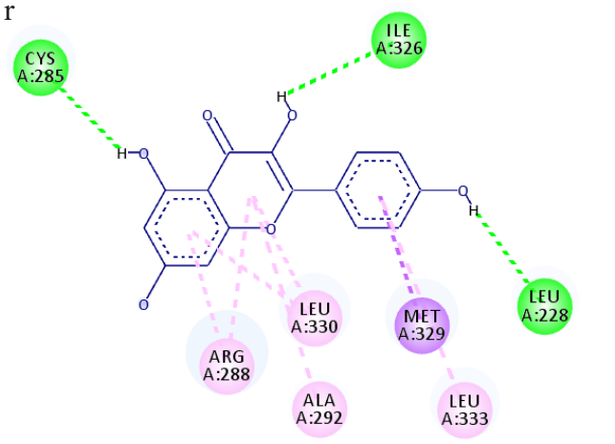
CYS
A:285
ILE
A:326
LEU
A:330
MET
A:329
LEU
A:228
ARG
A:288
ALA
A:292
LEU
A:333
Interactions
Conventional Hydrogen Bond
Pi-Sigma
Pi-Alkyl

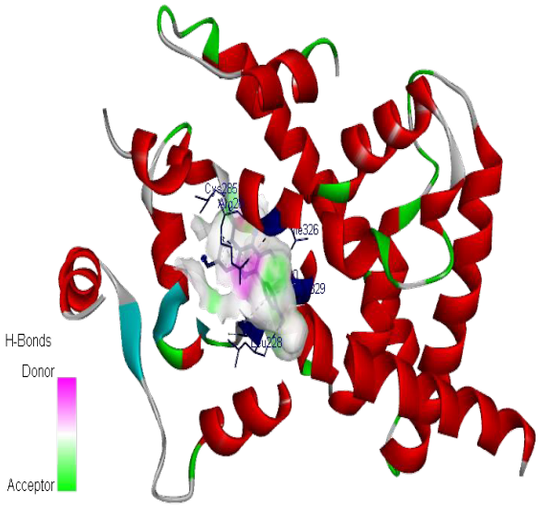
H-Bonds
Donor
Acceptor

s

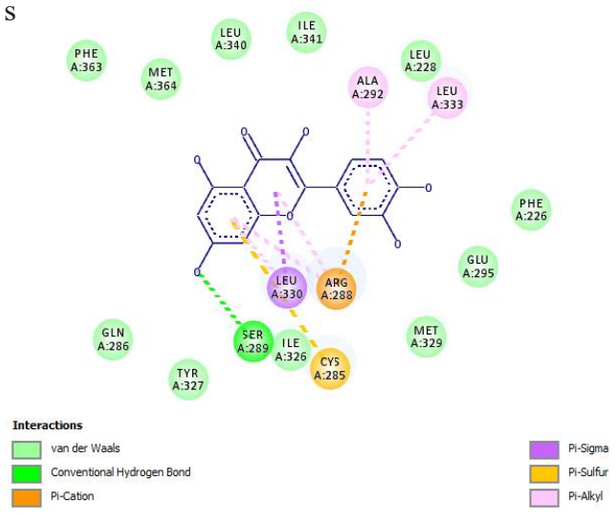
LEU
A:340
ILE
A:341
PHE
A:363
MET
A:364
LEU
A:228
ALA
A:292
LEU
A:333
PHE
A:226
GLU
A:295
LEU
A:330
ARG
A:288
GLN
A:286
SER
A:289
ILE
A:326
MET
A:329
CYS
A:285
TYR
A:327
Interactions
van der Waals
Conventional Hydrogen Bond
Pi-Cation
Pi-Sigma
Pi-Sulfur
Pi-Alkyl

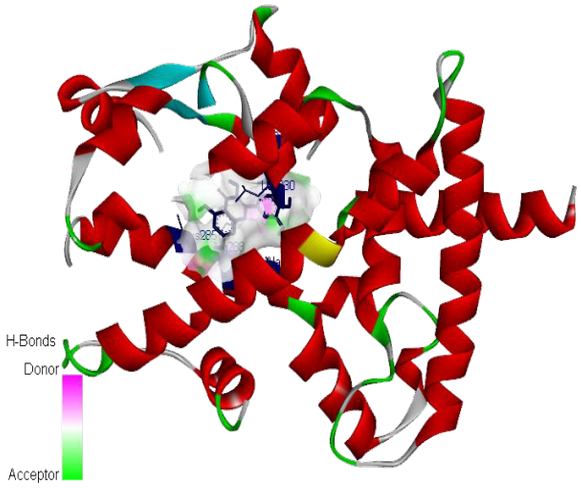
H-Bonds
Donor
Acceptor

t

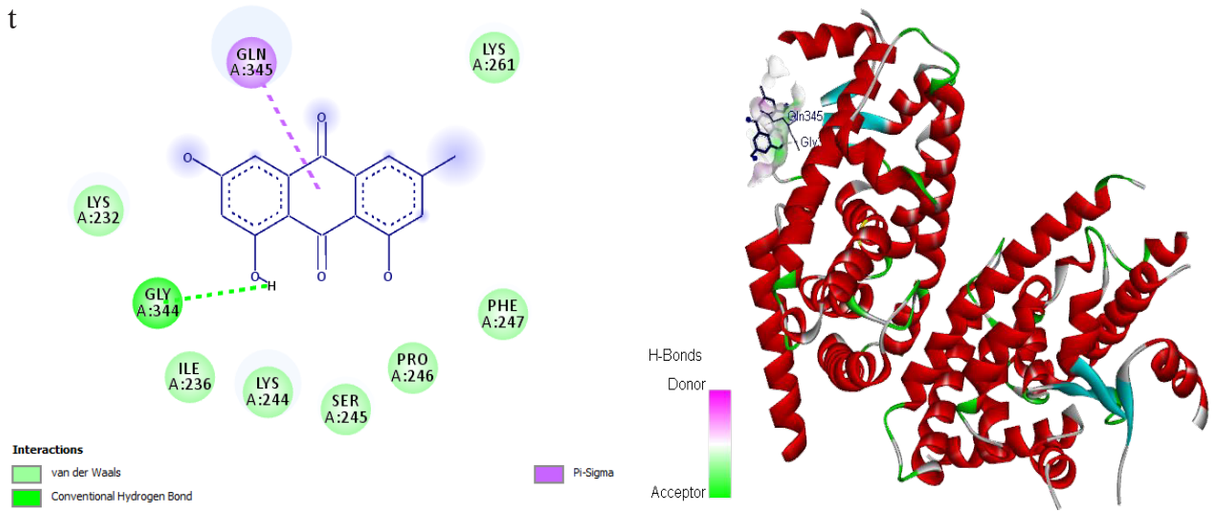
GLN A:345
LYS A:261
LYS A:232
GLY A:344
PHE A:247
PRO A:246
ILE A:236
LYS A:244
SER A:245
Interactions
van der Waals
Conventional Hydrogen Bond
Pi-Sigma
H-Bonds
Donor
Acceptor

u

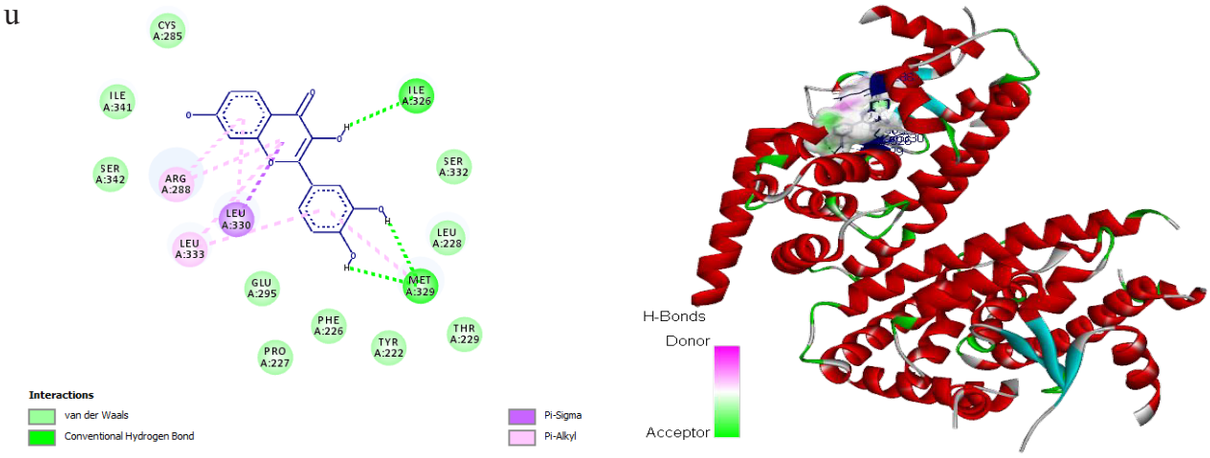
CYS A:285
ILE A:341
ILE A:326
SER A:342
ARG A:288
SER A:332
LEU A:330
LEU A:333
LEU A:228
GLU A:295
MET A:329
PHE A:226
THR A:229
TYR A:222
PRO A:227
Interactions
van der Waals
Conventional Hydrogen Bond
Pi-Sigma
Pi-Alkyl
H-Bonds
Donor
Acceptor

v

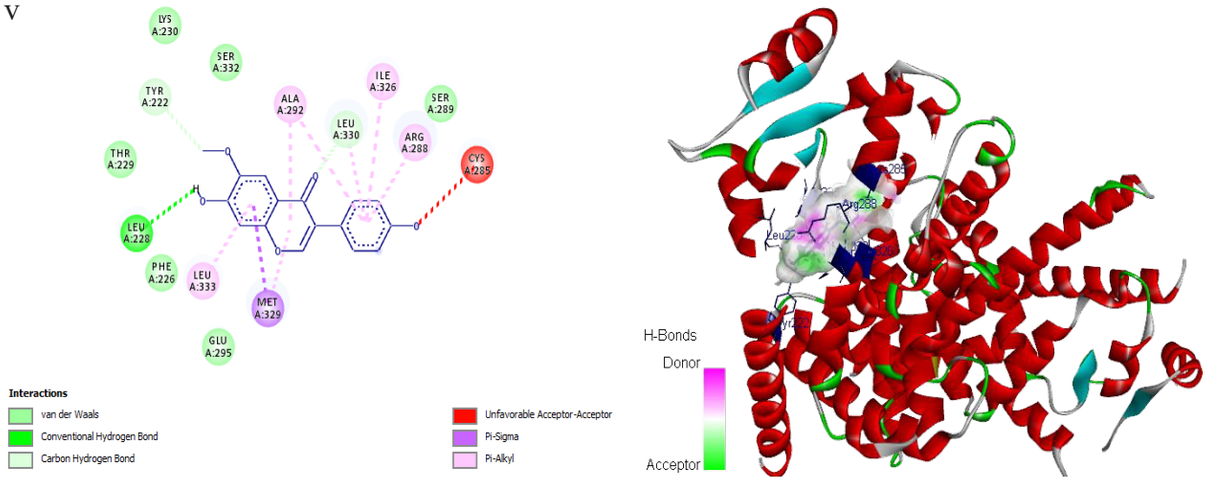
LYS A:230
SER A:332
TYR A:222
ALA A:292
ILE A:326
SER A:289
LEU A:330
ARG A:288
THR A:229
CYS A:285
LEU A:228
PHE A:226
LEU A:333
MET A:329
GLU A:295
Interactions
van der Waals
Conventional Hydrogen Bond
Carbon Hydrogen Bond
Unfavorable Acceptor-Acceptor
Pi-Sigma
Pi-Alkyl
H-Bonds
Donor
Acceptor

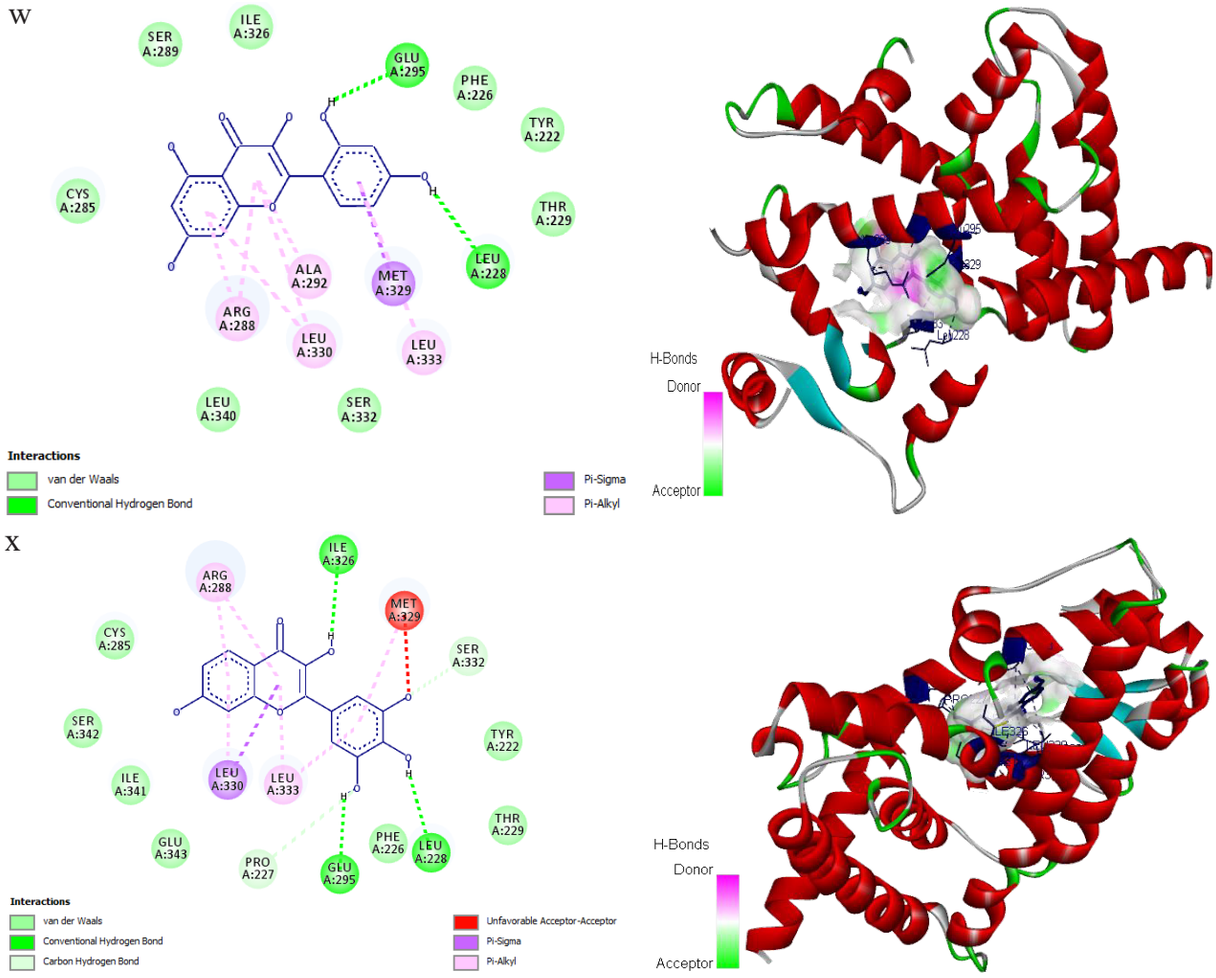


FIGURE S2. Docking compounds in 2D and 3D. Compounds of p-Coumaric acid (a), methyl nicotinate (b), and cinnamic acid (c) with HCAR2; muricatacin (d) with HMGCR; coronin (e), (-)-loliolide (f), and (+)-isololiolide (g) with PTGS2; coclaurine (h), anomuricine (i), (+)-anomurine (j), and anomurine (k) with ADRB3; coclaurine (l), anomuricine (m), (+)-anomurine (n), anomurine (o), and N-methylcoclaurine (p) with ADRB2; (Z)-3-Hexenyl beta-D-glucopyranoside (q) with VEGFA; chaempherol (r), quercetin (s), emodin (t), fisetin (u), glycitein (v), morin (w), and robinetin (x) with XDH